Blink-Perturbed Saccades in Monkey. II. Superior Colliculus Activity

H.H.L.M. GOOSSENS[1,2] AND A. J. VAN OPSTAL[1]
[1]*Department of Medical Physics and Biophysics, University of Nijmegen, NL-6525 EZ Nijmegen; and* [2]*Departments of Physiology and Anatomy, Erasmus University Rotterdam, NL-3000 DR Rotterdam, The Netherlands*

Goossens, H.H.L.M. and A. J. Van Opstal. Blink-perturbed saccades in monkey. II. Superior colliculus activity. *J Neurophysiol* 83: 3430–3452, 2000. Trigeminal reflex blinks evoked near the onset of a saccade cause profound spatial-temporal perturbations of the saccade that are typically compensated in mid-flight. This paper investigates the influence of reflex blinks on the discharge properties of saccade-related burst neurons (SRBNs) in intermediate and deep layers of the monkey superior colliculus (SC). Twenty-nine SRBNs, recorded in three monkeys, were tested in the blink-perturbation paradigm. We report that the air puff stimuli, used to elicit blinks, resulted in a short-latency (~10 ms) transient suppression of saccade-related SRBN activity. Shortly after this suppression (within 10–30 ms), all neurons resumed their activity, and their burst discharge then continued until the perturbed saccade ended near the extinguished target. This was found regardless whether the compensatory movement was into the cell's movement field or not. In the limited number of trials where no compensation occurred, the neurons typically stopped firing well before the end of the eye movement. Several aspects of the saccade-related activity could be further quantified for 25 SRBNs. It appeared that *1*) the increase in duration of the high-frequency burst was well correlated with the (two- to threefold) increase in duration of the perturbed movement. *2*) The number of spikes in the burst for control and perturbed saccades was quite similar. On average, the number of spikes increased only 14%, whereas the mean firing rate in the burst decreased by 52%. *3*) An identical number of spikes were obtained between control and perturbed responses when burst and postsaccadic activity were both included in the spike count. *4*) The decrease of the mean firing rate in the burst was well correlated with the decrease in the velocity of perturbed saccades. *5*) Monotonic relations between instantaneous firing rate and dynamic motor error were obtained for control responses but not for perturbed responses. And *6*) the high-frequency burst of SRBNs with short-lead and long-lead presaccadic activity (also referred to as burst and buildup neurons, respectively) showed very similar features. Our findings show that blinking interacts with the saccade premotor system already at the level of the SC. The data also indicate that a neural mechanism, rather than passive elastic restoring forces within the oculomotor plant, underlies the compensation for blink-related perturbations. We propose that these interactions occur downstream from the motor SC and that the latter may encode the desired displacement vector of the eyes by sending an approximately fixed number of spikes to the brainstem saccadic burst generator.

INTRODUCTION

In the companion paper (Goossens and Van Opstal 2000), we reported that blinking affects various aspects of saccadic behavior in monkey. It appeared that air-puff-evoked blinks had a considerable influence on both the kinematics and the spatial trajectories of saccadic eye movements. When elicited before saccade onset, these reflex blinks also reduced the saccade latencies substantially. Despite the strong disruptive nature of the evoked blinks, visually elicited saccades remained quite accurate in the absence of visual feedback. These behavioral data support the idea that blinking interferes with the saccadic premotor system and that an active control system may compensate for the blink-related perturbations. The neural mechanisms underlying these saccade-blink interactions, however, have so far received little attention in the literature and are difficult to assess on the basis of behavioral data alone.

Up to now, neurophysiological experiments have shown that the tonic activity of brain stem omnipause neurons (OPNs) pauses during blinks as well as saccades (Cohen and Henn 1972; Fuchs et al. 1991; Mays and Morrisse 1994), thereby disinhibiting saccadic burst neurons in the pontomedullary brain stem. These findings suggest that OPNs mediate, at least partly, the tight latency coupling between saccades and blinks. However, as discussed in the companion paper (Goossens and Van Opstal 2000) and in view of current models of saccade generation, the changes in both the trajectory and the kinematics of blink-perturbed saccades cannot be simply ascribed to an interaction at this premotor level. Moreover, a linear superposition of saccade- and blink-related signals at the extraocular motoneurons cannot readily account for the observed saccade behavior either. It is conceivable therefore that blinking affects other premotor stages of the saccadic system as well.

Recent studies indeed hint at the possibility that also the midbrain superior colliculus (SC) could be an important site of saccade-blink interactions. For example, both in rats (Basso et al. 1996) and in monkeys (Gnadt et al. 1997), it has been observed that electrical microstimulation of the SC transiently reduces the magnitude of air-puff-evoked blinks. As in rats (Basso and Evinger 1996), the monkey SC presumably excites a nonsaccadic pathway that inhibits the reflex blink circuitry (Gnadt et al. 1997). However, it is still unknown whether blinking affects the discharge patterns of saccade-related collicular neurons and how this could in turn affect saccade generation. In the present paper, we therefore studied single-unit activity in the intermediate and deep layers of the SC with the use of the blink-perturbation paradigm.

It is well established that the SC has extensive projections to saccadic burst cells in the pontomedullary brain stem and that the SC is critically involved in the generation of normal saccadic eye movements (see e.g., Moschovakis and Highstein 1994; Sparks and Hartwich-Young 1989 for reviews). Many neurons in its intermediate and deep layers generate a burst of activity just before and during saccades directed to a particular

The costs of publication of this article were defrayed in part by the payment of page charges. The article must therefore be hereby marked "*advertisement*" in accordance with 18 U.S.C. Section 1734 solely to indicate this fact.

region of the visual field, referred to as the movement field of the neuron. Together, these saccade-related burst neurons (SRBNs) form a topographically organized motor map in which anatomically nearby cells have overlapping movement fields (Lee et al. 1988; Mays and Sparks 1980; McIlwain 1982; Ottes et al. 1986; Robinson 1972; Schiller and Stryker 1972).

Until recently, it was generally held that the amplitude (R) and direction (Φ) of an impending saccade is specified by the *location* of the active cell population in the SC motor map rather than by the *temporal* discharge patterns of the recruited neurons. Several studies have suggested, however, that the collicular output may also determine the kinematics and trajectory of the saccade (Berthoz et al. 1986; Lee et al. 1988; Munoz et al. 1991; Van Opstal et al. 1990; Waitzman et al. 1991; Wurtz and Optican 1994). These findings have led to new quantitative models that place the SC inside the so-called local feedback loop. This internal feedback circuit is thought to control the saccade trajectory by a continuous comparison of the desired eye displacement signal with an internal representation (efference copy) of the actual eye displacement during the saccade (e.g., Arai et al. 1994; Droulez and Berthoz 1991; Lefèvre and Galiana 1992; Optican 1995; Van Opstal and Kappen 1993). Previously most models assumed that the local feedback loop is closed through assemblies of cells in the pontomedullary brain stem (Jürgens et al. 1981; Scudder 1988; Van Gisbergen et al. 1981).

A difficulty in studying the role of the SC in the control of saccades is the stereotyped relationship between the amplitude of normal saccades and their duration and peak velocity (referred to as the "main sequence") (Bahill et al. 1975; Fuchs 1967). In an attempt to overcome this problem, previous saccade-interruption paradigms have used intrasaccadic microstimulation of either the OPNs (Keller and Edelman 1994) or of the rostral SC (Munoz et al. 1996). In these experiments, it was found that the microstimulation not only stopped the eye in saccade mid-flight, but it also induced a brief pause in the discharge of collicular SRBNs. Shortly after the stimulation ended, the saccade resumed its course, and the same population of SC cells that was active before the stimulation was reactivated even though the resumed movement did not belong to the movement field of these cells. By contrast no, or only minimal, activity was found in cells whose movement field optimum matched the metrics of the resumed saccades. By what mechanism the same neurons are reactivated is still unclear. One possible explanation is local feedback, which indeed predicts a resumed discharge (e.g., Arai et al. 1994). The finding that the SRBN discharge rate during the resumed saccades still showed the same monotonic relation with the remaining motor error than the one obtained for uninterrupted saccades further supported this hypothesis (e.g., Das et al. 1995).

However, a problem that still hampers the interpretation of the saccade-interruption data are the stereotyped kinematics of the resumed movements and the lack of a change in eye-movement direction. Moreover, the potential danger of stimulating adjacent oculomotor pathways, both upstream and downstream from the SC, makes the interpretation of stimulation data less obvious then at first glance. For example, OPN and rostral SC stimulation not only stopped the saccade in mid-flight, but it also interrupted the SRBN discharge. Hence it appeared that the SRBNs did not represent the remaining motor error during the interruption period. It is unclear, however, whether the cessation of SRBN discharge could be a side effect of the electric stimulation. It is ambiguous therefore whether the SRBNs *detected* the perturbation (through feedback) or whether they instead *caused* the interruption of the saccade. By imposing natural perturbations on the saccadic system that affect both the kinematics and spatial trajectories of saccadic eye movements, the blink-perturbation paradigm may offer an opportunity to circumvent these difficulties.

In view of current models of the SC and the notion of local feedback control, the present paper investigates how blink-related spatial-temporal perturbations of the saccade trajectory are reflected in the SC activity patterns. A preliminary account of these experiments has been presented in abstract form (Goossens et al. 1996; Van Opstal and Goossens 1999).

METHODS

Subjects

The neurophysiological data presented in this paper were obtained from three rhesus monkeys (*Macaca mulatta*) and were collected during the behavioral experiments described in the companion paper (Goossens and Van Opstal 2000). Details about the setup, surgical procedures, and methods used to measure eye and eyelid position as well as the applied behavioral paradigms, are described in that paper. Here we provide only a brief summary, and additional methods that were used to record and analyze the single-cell activity. All experiments were conducted in accordance with the European Communities Council Directive of November 24, 1986 (86/609/EEC) and were approved by the local university ethics committee.

Apparatus

The head-restrained monkeys were seated in a primate chair facing an array of 85 light-emitting diodes (LEDs) in an otherwise completely dark room. The horizontal and vertical components of the left eye position were measured with the double-magnetic-induction technique (Bour et al. 1984). Movements of the contralateral right eyelid were measured with the magnetic search-coil induction technique (Collewijn et al. 1975) by taping a small coil on the eyelid. Air puffs (20 ms, 1.4–1.8 Bar) were generated by a pressure unit and presented on the recording eye to elicit trigeminal blink reflexes.

The activity of single units was recorded with glass-coated tungsten microelectrodes (0.2–1.2 MΩ) that were positioned in the SC using a hydraulic stepping motor (Trent Wells). The latter was mounted on the stainless steel recording chamber that was placed above a trephine hole at stereotaxic coordinates [AP, RL] = [0,0] and aimed at the SC. The electrode signal was amplified (Bak Electronics, Model A-1), low-pass filtered (15 kHz), and monitored on an oscilloscope. Action potentials were detected by a level detector and discriminated on the basis of their waveforms using a real-time decomposition of the first four principal components (e.g., Epping and Eggermont 1987). The accepted spike events were subsequently fed into a four-bit spike counter, which produced a stepwise DC output that was sampled at a rate of 1 kHz. This ensured that no spikes were missed, irrespective of the instantaneous discharge rate during vigorous bursts of action potentials.

SC localization and histology

The in vivo localization of the SC was based on the following criteria: *1*) the stereotaxic coordinates of the recording sites corresponded closely to the coordinates of the SC as given by Snider and Lee (1961). The size of the area with visual- and saccade-related activity was also in accordance with this atlas. *2*) A region without action potentials, corresponding to the superior cistern, was often

passed before the electrode entered the superficial layers of the SC. Usually the upper boundary of the SC was readily recognized by the activity of visual neurons with limited contralateral receptive fields and response latencies of ~70 ms. *3*) At deeper locations, typically between ~0.8 and 3 mm below the SC surface, clear saccade-related activity was encountered. In these layers, electrical stimulation with pulse trains (25 negative pulses of 0.5-ms duration at 500 Hz) at low current strengths (20–50 μA) evoked reproducible saccades that corresponded well with the movement fields of nearby saccade-related neurons. The latencies of stimulation-evoked saccades were ~20 ms, and thresholds for evoking saccades were typically <10 μA. *4*) The topographic motor map of the SC (Robinson 1972) could reliably account for the optimal saccade vector of cells encountered in subsequent penetrations. And *5*) after further lowering of the electrode, sustained auditory-evoked responses with short latencies, indicative for the inferior colliculus, were often encountered (Goossens et al. 1997).

After completing the experiments, two of the monkeys (*SA* and *ER*) were deeply anesthetized with an overdose of pentobarbital and perfused directly through the internal carotid artery with 2 l phosphate-buffered saline, pH 7.4, at 37°C, followed by 2 l of fixative containing phosphate-buffered 2% paraformaldehyde and 2.5% glutaraldehyde, pH 7.4. Immediately after perfusion, the midbrain was dissected out. Serial cryostat sections were made and prepared for standard histology (Nissl staining). Examination of the midbrain sections at low and high magnification showed that the penetrations were made through the SC. Most of the penetrations reached the intermediate and deep layers.

Experimental protocol

After isolating an SRBN, saccades were evoked toward all LEDs of the target array. These data were used for accurate calibration of the eye-position signals (see Goossens and Van Opstal 2000) and to estimate the location and extent of the cell's response field. Subsequently, the movement field of the neuron was characterized in detail by eliciting saccades to a series of targets presented inside and neighboring the cell's response field.

A typical *movement field scan* consisted of 85 different fixation/target configurations: 5 different target positions and 17 different initial fixation positions (usually within 5° from the center LED), yielding a spatial resolution down to 0.5°. In each trial, the monkey first looked a fixation spot that was presented for 800–1,600 ms (randomized). Then as soon as the fixation spot disappeared, a peripheral target was presented for another 900 ms at a pseudo-randomly selected location that the animal refixated with a saccade. When a better dissociation between visual- and saccade-related activity was required, the saccade latencies were increased by presenting the target 100 ms prior to the offset of the fixation point (overlap paradigm) (Fischer and Weber 1993).

After this standard procedure, which was usually repeated near the end of a recording session, the neuron's activity was tested with the use of the *blink-perturbation paradigm* that has been described in the companion paper (Goossens and Van Opstal 2000). In short, saccades were made in complete darkness from a fixation point to either one of five randomly selected and briefly flashed (50 ms) peripheral targets, typically into the central region of the cell's movement field. In 30% of the trials, air puffs were presented at a fixed moment after target onset (between 120 and 180 ms) to elicit a reflex blink (mean latency ~20 ms) near the onset of the saccade. Control and perturbation trials were randomly interleaved with catch trials. In the latter trials, target positions were chosen such that the evoked saccades could be matched to the successive eye-movement components of perturbed responses (see RESULTS, Fig. 11). Cells were also tested with the use of the *fixation-blink paradigm*, in which air-puff-evoked blinks were elicited while the animal attempted to fixate a straight-ahead fixation spot (see Goossens and Van Opstal 2000).

Data analysis

For details regarding saccade and blink detection procedures as well as statistic criteria that were used to discriminate between compensatory and noncompensatory responses, the reader is referred to METHODS and RESULTS of the companion paper (Goossens and Van Opstal 2000).

The raw single-cell activity was displayed in spike rasters aligned on specific events such as target onset, air puff onset, the onset or offset of a saccade, or the onset of a blink. All neurons that showed a sharp increase in their activity slightly preceding (~20 ms) and tightly linked to the onset of saccades directed into their movement field were considered saccade-related and were therefore subjected to further analysis. The location and extent of a cell's movement field was determined from the movement field scan data by plotting the number of spikes, counted from 20 ms before saccade onset to saccade offset, as function of saccade amplitude and direction. Quantitative descriptions of the movement fields were obtained by fitting two-dimensional Gaussian activation profiles to the cells' activity as function of saccade vectors in collicular motor map coordinates (see Ottes et al. 1986 for extensive details) (goodness of fit: r typically between 0.85 and 0.98).

The raw spike trains were converted into smoothed representations of a cell's instantaneous firing rate by constructing spike density functions (*D*). To that end, all spike events in a trial were substituted by Gaussian pulses of width $\sigma = 4$ ms and height $1/(\sigma\sqrt{2\pi})$ and summed to produce a continuous function of time (MacPherson and Aldridge 1979; Richmond and Optican 1987). Large values of the spike density function represent a high probability of spike occurrence, and the peak of the function represents the peak discharge of the cell (in spikes/s). To estimate the duration of the saccade-related burst during individual saccades more robustly, the width of the Gaussian was increased to $\sigma = 10$ ms (see RESULTS).

Dynamic motor error (*ME*) was defined as the difference between saccade endpoint and instantaneous eye position. The average phase relations between spike density and dynamic motor error shown in Figs. 12, *C–E*, and 13, *A–F*, were obtained by averaging the spike density and dynamic motor error signals as function of time for series of matched eye movements. It was not always possible, however, to find a sufficient number of perturbed responses with closely matched movement profiles. To circumvent this problem, the spike density function of each trial was resampled as function of the declining radial motor error using spline interpolation. In this way, all responses with matched saccade amplitudes and directions could be used to compute the average phase relations for each neuron in Fig. 13, *G* and *H*, despite the large variability in movement kinematics.

RESULTS

Single-unit activity was recorded from a series of SRBNs encountered in the intermediate and deep layers of the SC of three monkeys. Twenty-nine of these neurons (*PJ*: $n = 17$; *SA*: $n = 4$; *ER*: $n = 8$) were studied with the use of the blink-perturbation paradigm in which visually evoked saccades were disturbed by air-puff-evoked reflex blinks. Of the 29 SRBNs tested, 25 neurons remained isolated long enough to obtain a full 2-D scan of their movement field as well as a sufficient series of perturbed saccades for the quantitative analysis described in the following text. For the remaining four cells, we gathered sufficient data in at least the blink-perturbation paradigm to verify that they showed qualitatively similar features to the more thoroughly studied set of 25 SRBNs.

Isolated collicular neurons were classified as SRBNs if they showed a sharp increase in their firing rate ~20 ms before and tightly linked to the onset of saccades directed into the cell's

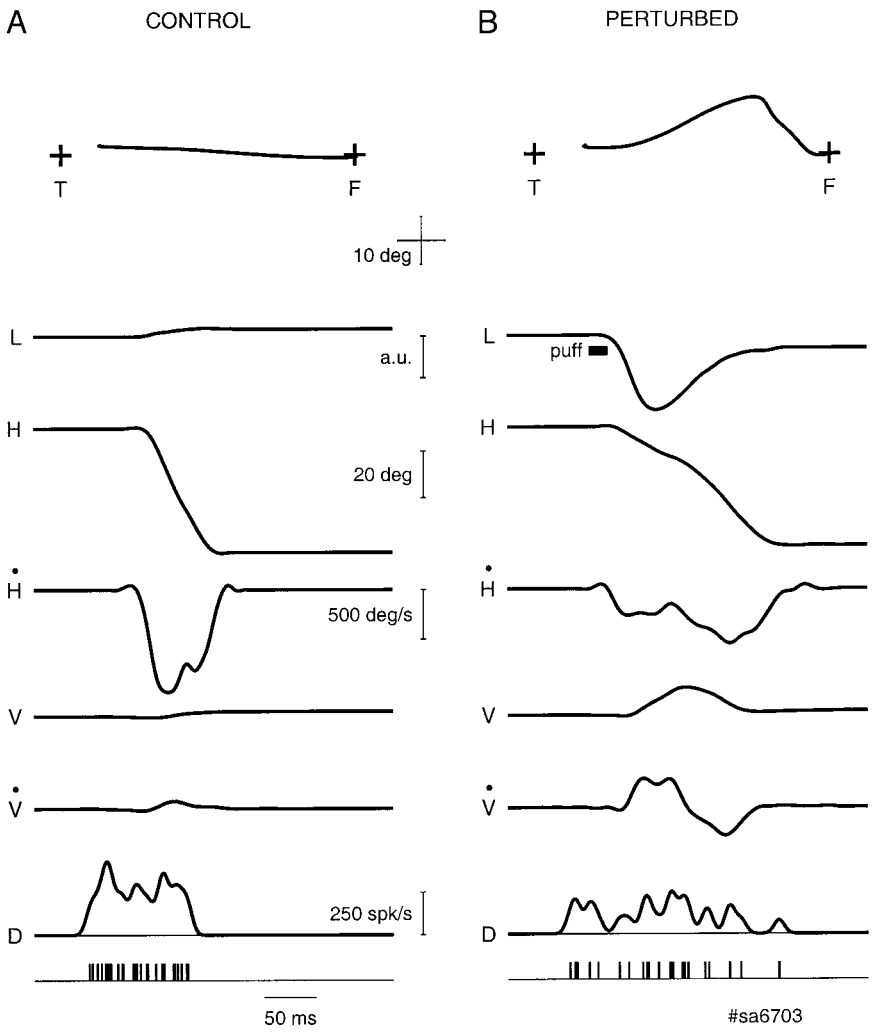

FIG. 1. Typical example of the persistent burst discharge of a collicular saccade-related burst neuron (SRBN) for a saccade that was perturbed by an air-puff-evoked reflex blink. Activity of this neuron (*sa6703*) was recorded during a control saccade (*A*) and during a blink-perturbed saccade (*B*) of comparable amplitude and direction ([*R*, Φ] = [60, 0] deg). Both movements were evoked from the fixation point (*F*) toward the briefly (50 ms) flashed target (*T*). Spatial trajectories of the 2 saccades are shown at the *top*. Subsequent traces show vertical eyelid position (*L;* in arbitrary units), eye position (*H*, horizontal and *V*, vertical; in °), and eye velocity (*H*, horizontal and *V*, vertical; in °/s). As in all subsequent figures, eyelid movements were recorded from the contralateral, unstimulated eye. Bottom traces show spike density (*D;* σ = 4 ms; in spikes/s; see METHODS), as well as the individual action potentials (vertical lines). The neuron's optimum was at, or beyond 60° to the left.

movement field, irrespective of other pre- and postsaccadic discharge properties. In saccade trials, most of the cells (25/29) also showed a brief visual response ~70 ms after the visual stimulus appeared inside their receptive field. A prelude of presaccadic activity that could start several tens of milliseconds before the high-frequency, saccade-locked burst was also frequently observed. Cells that were endowed with a considerable amount of long-lead (>100 ms) presaccadic activity also showed a considerable amount of postsaccadic activity over a period of 100 ms after the saccade and were typically encountered at deeper locations from the SC surface. Saccade amplitudes for which the recorded SRBNs were maximally recruited ranged between 8 and 50°, except for four cells in the caudal SC which had no optimum for saccade amplitudes <70°. When tested in fixation trials, SRBNs were silent, and they were not recruited when air puff stimuli were presented in fixation-blink trials.

Activity during compensatory saccades

When air puffs were used to elicit a reflex blink near the onset of saccades, not only were the stereotyped spatial-temporal properties of saccades disturbed (Goossens and Van Opstal 2000) but the discharge patterns of SRBNs in the SC also were clearly modified. This is illustrated in Fig. 1, which compares the discharge of a saccade-related neuron (*sa6703*) in the caudal SC during a control saccade (~60° to the left; Fig. 1*A*) and during a blink-perturbed saccade that landed close to the extinguished target (Fig. 1*B*). Figure 1*B* shows, in a qualitative way, the consistent features of blink-perturbed responses that were obtained in all three monkeys. First, at the onset of the blink, the eye rapidly deviated from its normal, straight trajectory (typical latencies ~20 ms relative to the air puff onset at the eye), and no sharp increase in the cell's discharge was observed around the eye-movement onset. Second, as the cell continued its low-level discharge, the eye movement continued, and the perturbation in both direction and velocity was compensated in complete darkness. Finally, the increase in movement duration to reach the target was matched by a comparable increase in the duration of the cell's discharge.

To document the reproducibility of these findings among our sample of collicular neurons, Figs. 2 and 3 show the activity of two other representative SRBNs during a series of control trials and a series of perturbation trials. The data plotted in Fig. 2 were recorded from a neuron (*pj5203*) that was found in the central region of the SC motor map. Saccade vectors were matched in amplitude and direction, and data are aligned on different events, from *top* to *bottom*: saccade onset (Fig. 2,

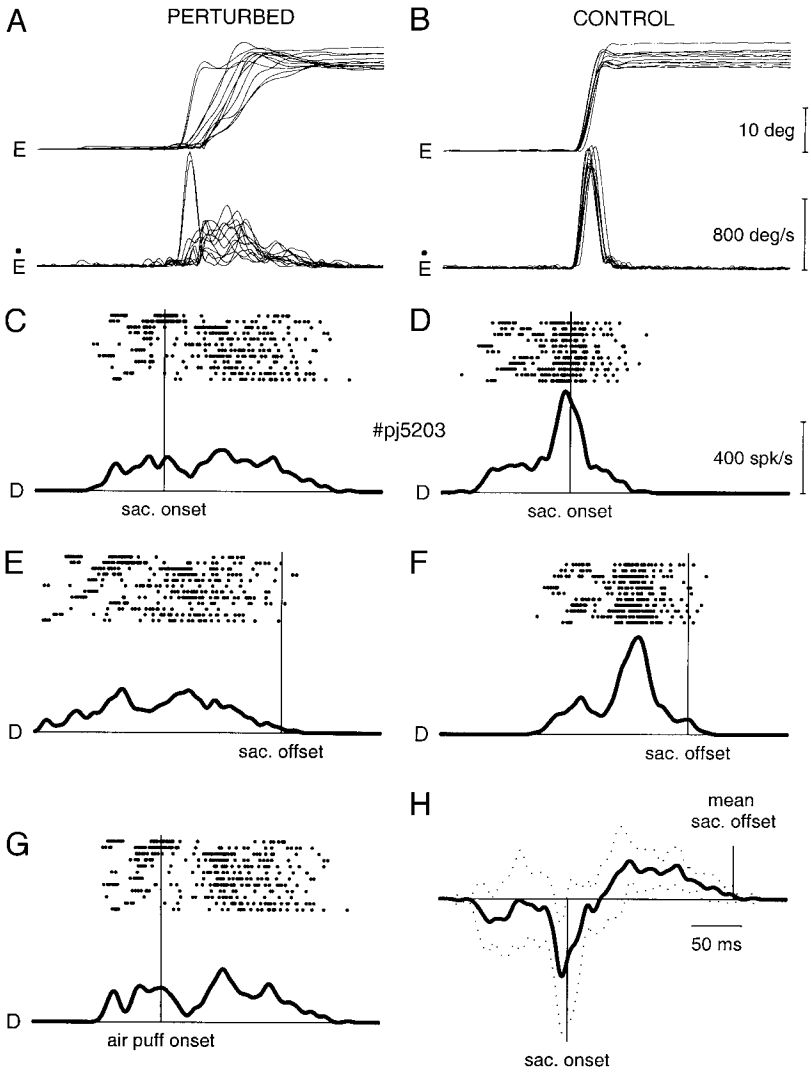

FIG. 2. Clipped activity of an SRBN (*pj5203*) for a series of perturbed and control saccades made in darkness toward the position of targets flashed at [*R*, Φ] = [20, 60] deg. Amplitude and direction of the saccade vectors were matched and corresponded closely to the cell's optimum. *A* and *B*: radial eye position ($E = \sqrt{H^2 + V^2}$) and vectorial eye velocity ($E = \sqrt{\dot{H}^2 + \dot{V}^2}$) traces. Subsequent panels show spike rasters and averaged spike density aligned with saccade onset (*C* and *D*) with saccade offset (*E* and *F*) and with air puff onset in the perturbation trials (*G*), respectively. *H*: comparison of the cell's discharge during perturbed saccades and control saccades by showing the difference in the average spike-density waveforms when data were aligned with saccade onset. ···, standard deviation. The cell's burst discharge during perturbed saccades is consistently prolonged until the movement ends, and a transient suppression of activity, shortly after the air puff onset, is apparent. Note the 2 trials where the perturbation occurred late in the saccade (*top rows* in the spike rasters).

A–D), saccade offset (Fig. 2, *E* and *F*), and air puff onset (Fig. 2*G*). As shown in Fig. 2, *right*, the cell showed a brisk burst discharge for control saccades of optimal amplitude and direction ([*R*, Φ] = [20, 60] deg). The onset of the saccade-related burst ("motor burst" for short) preceded the saccade onset by ~20 ms (Fig. 2*D*) and peaked shortly before saccade onset. Subsequently the discharge declined sharply during the saccade until it stopped when the saccade ended (Fig. 2*F*). Neurons with such behavior have also been referred to as clipped burst neurons (Munoz and Wurtz 1995; Waitzman et al. 1991). During perturbation trials (Fig. 2, *left*), the cell's burst discharge was clearly disturbed along with the saccade kinematics. As may be observed in Fig. 2*C*, the neuron typically showed an irregular discharge around movement onset, except in two trials where the cell showed a near-normal burst (*top rows* of the spike rasters). The irregular, lower-frequency discharge was associated with the low-velocity saccades, whereas the two clear bursts were associated with the two high-velocity saccades (clearly identifiable in Fig. 2*A*). Figure 2*G* shows the same responses aligned with air puff onset. Note that the cell's (upcoming) burst activity was transiently suppressed shortly after the air puff arrived at the eye. About 30–40 ms after the air puff onset, the cell resumed its activity, and it continued its discharge until the perturbed saccade ended. The latter can be readily observed in Fig. 2*E*, which shows the data aligned with saccade offset. Figure 2*H* compares the two conditions by showing the difference between the average spike-density function for control and perturbed trials (data aligned with eye-movement onset). As was typically observed, the resulting difference waveform was endowed with an initial negative component, followed by a positive phase that ended with the average end of perturbed saccades. The biphasic profile illustrates both the initial suppression as well as the prolongation of the cell's burst discharge in the perturbed condition. Note that the negative component leads the eye-movement onset because the air puff typically preceded the onset of the impending saccade, thereby interfering already with the cell's presaccadic discharge.

Figure 3 shows comparable data obtained from an SRBN (*er1101*) that was endowed with long-lead presaccadic activity. As may be observed in Fig. 3*D*, this prelude activity was followed by a more intense burst just before and during control saccades of optimal amplitude and direction ([*R*, Φ] = [14, 150] deg). The discharge peaked at saccade onset and then declined rapidly toward the end of the saccade. After this high-frequency burst, the neuron showed a gradual decline of

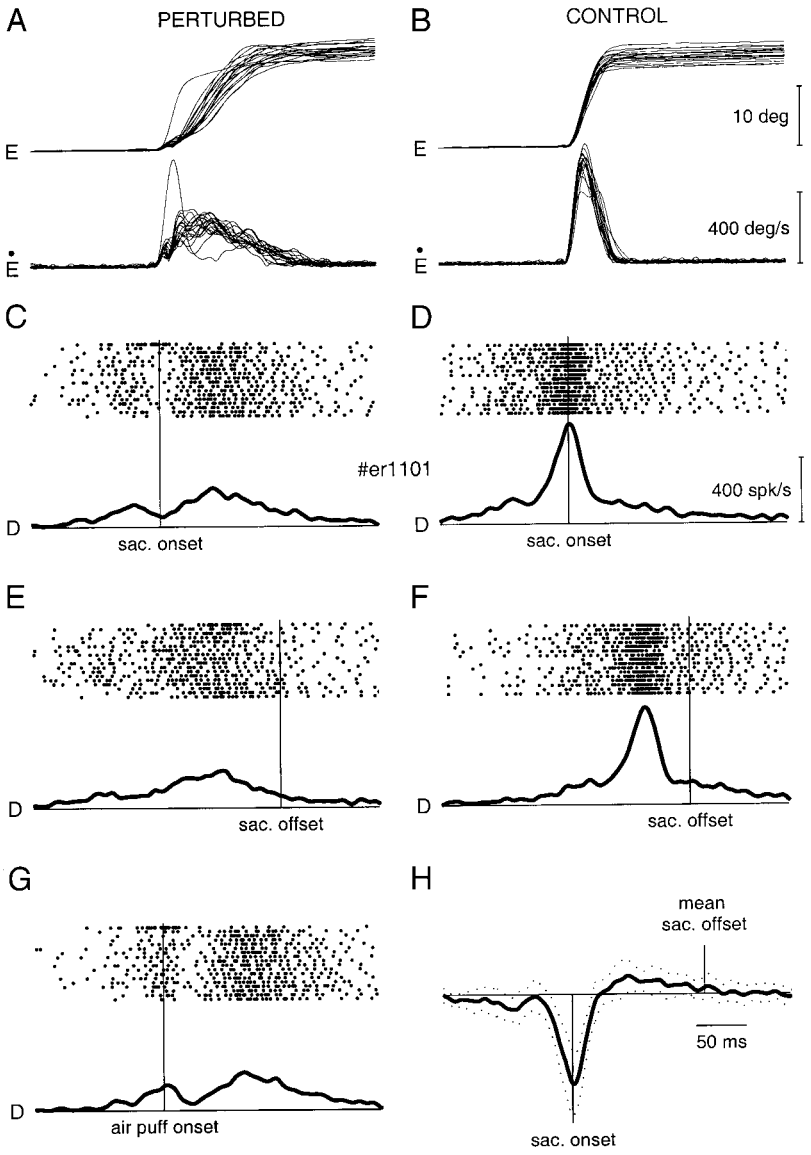

FIG. 3. Unclipped activity of an SRBN (*er1101*) in the blink-perturbation paradigm. Same display format as in Fig. 2. Note the buildup of presaccadic activity and the gradual decline of the postsaccadic activity. The neuron's optimum saccade vector was at $[R, \Phi] = [14, 150]$ deg. Apart from a substantial amount of intrinsic noise, the cell's response showed comparable features as the neurons with a clipped discharge presented in Figs. 1 and 2. Note the 1 trial with a late perturbation (*top row* in the spike rasters).

postsaccadic activity over a period of ~250 ms (i.e., unclipped discharge; see Fig. 3*F*). Collicular neurons that exhibit such temporal discharge characteristics have also been named buildup neurons (Munoz and Wurtz 1995). During perturbation trials (Fig. 3, *left*), the cell's activity was clearly suppressed within ~10–20 ms after the air-puff onset (Fig. 3*G*). As the air puffs were presented prior to the impending saccade, the onset of the suppression *preceded* the actual saccade onset (Fig. 3*C*), except in the one trial (*top row* of the spike raster) where the perturbation occurred toward the end of the saccade (see Fig. 3*A*). Following a near complete cessation of activity, the neuron resumed its discharge ~30–40 ms after the air-puff onset (Fig. 3*G*). Although the discharge of this neuron did not end at saccade offset, it may be inferred from the spike rasters in Fig. 3*E* that it showed an increased firing rate until the end of the perturbed eye movements. This prolongation of the cell's saccade-related activity is also evident from the difference between the average control and perturbed response (Fig. 3*H*), which drops to zero around the mean offset of the perturbed saccades.

Suppression and resumption of SRBN discharge

Since the air puffs often interfered already with the cells' *pre*-saccadic discharge, the impression was obtained that the changes in SRBN activity were the underlying cause rather than the consequence of modified saccade kinematics. To gain further insight into the possible mechanism that could underlie the suppression of SRBN discharge, we also examined responses in which the saccade was accompanied by a gaze-evoked blink. As shown in the companion paper (Goossens and Van Opstal 2000), the spatial-temporal perturbation resulting from gaze-evoked blinks were qualitatively similar to those obtained with air-puff-evoked blinks.

Figure 4 compares the responses of two different SRBNs that were recorded under both air-puff- and gaze-evoked blinking conditions. The two cells, *er0902* (Fig. 4, *A* and *B*) and *pj6802* (Fig. 4, *C* and *D*), were isolated in the left and right SC, respectively. Note that the burst activity of both cells was strongly suppressed following the onset of reflex blinks that were evoked by air puff stimulation of the left eye (Fig. 4, *A* and *C*). By contrast, no transient suppression was observed following

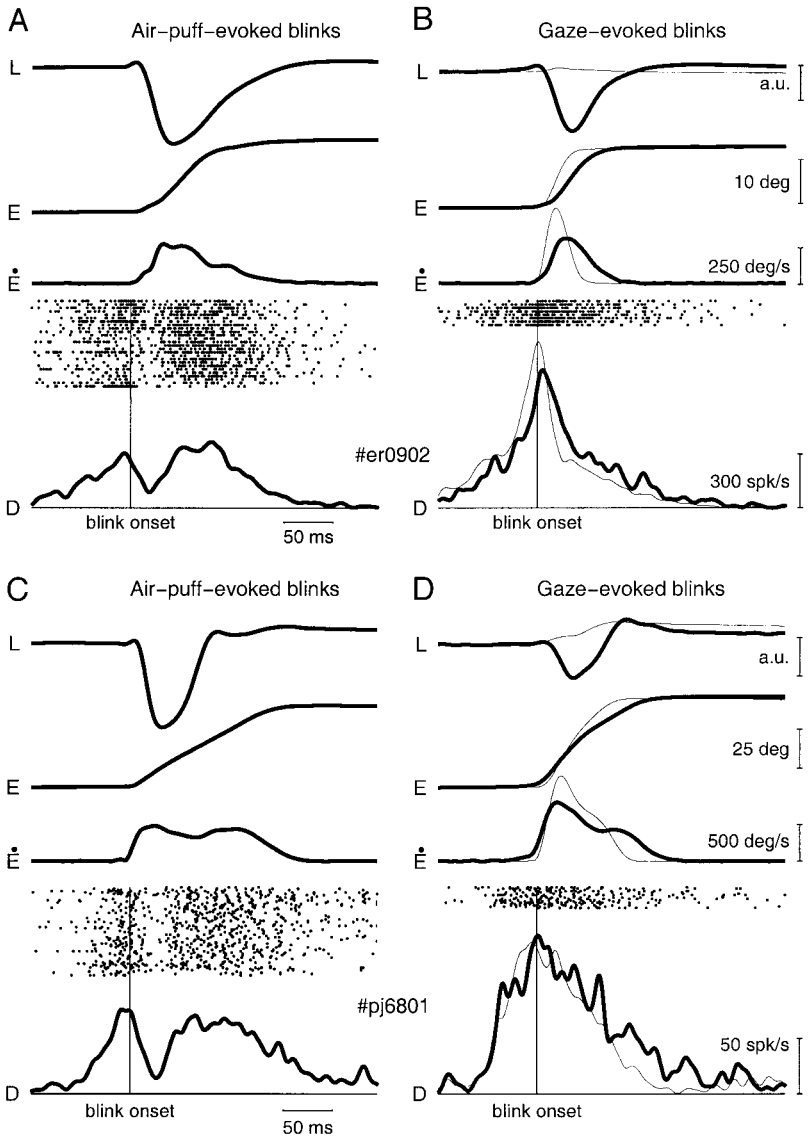

FIG. 4. Discharge of 2 different SRBNs under air-puff and gaze-evoked blinking conditions. *A* and *B*: SRBN found in the left superior colliculus (SC; *er0902*). *C* and *D*: SRBN found in the right SC (*pj6801*). Data were aligned to blink onset and averaged (thick traces). Average control responses are superimposed in *B* and *D* (thin traces). A strong transient suppression of activity following the onset air-puff-evoked blinks is apparent for both cells (*A* and *C*). By contrast, no transient suppression is observed in the case of gaze-evoked blinks (*B* and *D*). Note that the SRBN discharge as well as the saccade kinematics were only mildly affected in the case of gaze-evoked blinks.

the onset of gaze-evoked blinks (Fig. 4, *B* and *D*; thick traces), which had a comparatively small influence on the discharge of the SRBNs. Note that this difference in SRBN discharge is also reflected in the saccade kinematics, which were less dramatically disturbed by gaze-evoked blinks. The latter may be inferred from the control data that are superimposed in Fig. 4, *B* and *D* (thin traces). On average, also the air-puff- and gaze-evoked blinks were different. However, by selecting a subset of responses with comparable eyelid traces, it could be excluded that the differences in SRBN discharge were merely due to differences in blink magnitude (data not shown).

As illustrated by the preceding examples, SRBNs showed a transient decrease in their discharge following the onset of an air puff. Although present in most cells tested, this suppression was often far from complete and variable from trial to trial. Moreover, at the time of the air puff (fixed re. target onset, see METHODS), the amount of presaccadic activity was variable due to considerable scatter in the onset latencies of the motor burst with respect to target onset (see Fig. 4, *A* and *C*). It was not possible therefore to quantify the onset latency and the duration of this phenomenon for each neuron with the same accuracy.

To obtain at least a crude estimate of the time course of the suppression and subsequent resumption of SRBN activity, we analyzed the discharge of those SRBNs ($n = 7$) that exhibited a strong suppression in a large number of trials. To that end, the spike-density functions from all perturbation trials in a recording session, except the ones in which the perturbations occurred very early or very late in the burst, were averaged (n between 20 and 80; $\sigma = 4$ ms) and subsequently normalized with respect to the mean. Figure 5, *A* and *B*, shows the results of this procedure for each neuron (thin curves) when data were aligned to air puff onset and blink onset, respectively. Averaged data of the seven neurons (thick curves) are superimposed. As may be inferred from these data, the suppression starts, on average, ~10 ms after the air puff onset and leads the blink onset by an approximately similar amount. About 10–30 ms after the blink onset, the SRBNs resumed their discharge. Some caution is called for with regard to the interpretation of the data in Fig. 5*B* because movements of the contralateral, unstimulated eyelid were used to detect blink onsets. However, as indicated in the companion paper (Goossens and Van Opstal 2000), it is reasonable to assume that there is no significant

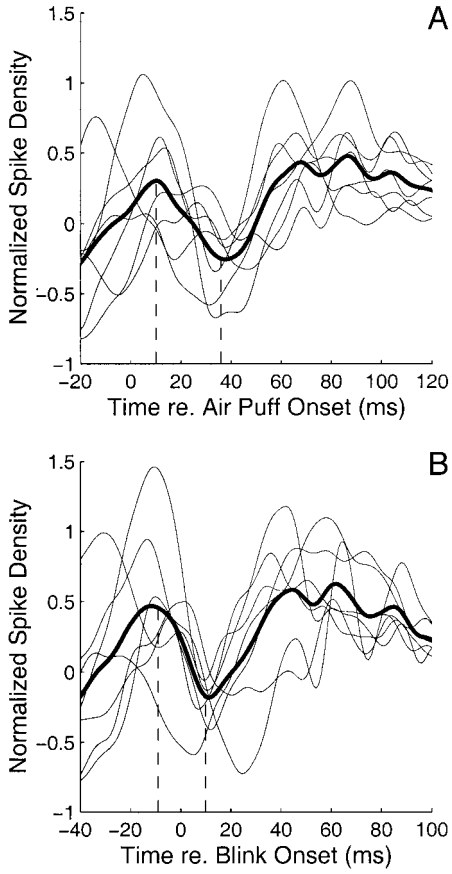

FIG. 5. Time course of the blink-related suppression and resumption of SRBN discharge. *A*: averaged and normalized spike density waveforms from 7 SRBNs (thin curves), aligned with air puff onset. Trials in which the perturbation occurred very early or very late in the burst were removed from the data sets. Each curve was normalized with respect to its mean. Although the precise onset of the suppression is ill defined for each neuron (see text), a crude estimate from the averaged cell data (thick curve) indicates a latency of ~10 ms relative to the air puff onset. *B*: same data as in *A*, but now the individual responses (n between 20 and 80) were aligned to the onset of the (consensual) blink. Note that the suppression starts, on average, ~10 ms before the blink onset. Approximately 10–30 ms after the blink onset, the neurons resumed their discharge.

latency difference between ipsi- and contralateral eyelid movements as the short-latency, uncrossed R1 component of the primate blink reflex hardly contributes to movements of the eyelid (Bour et al. 2000).

Quantitative analysis of the saccade-related discharge

Unlike in previous saccade interruption paradigms, the evoked perturbations in the present experiments typically affected the entire saccade. Nevertheless the data presented so far indicate that the response properties of SRBNs during blink-perturbed saccades showed qualitatively similar features as have been observed during interrupt saccades (Keller and Edelman 1994; Munoz et al. 1996). Therefore to facilitate a comparison between the interruption data and the present data set, we started out with a comparable quantitative analysis.

BURST DURATION. The raw data in Figs. 1–3 indicate that the SRBNs showed a prolonged burst discharge until the perturbed eye movement ended. To quantify this feature, we determined the duration of the motor burst for each individual saccade into the cell's movement field. For neurons showing clipped or partially clipped activity in the control condition ($n = 13$), the burst duration was measured from 20 ms before saccade onset to the time when the spike density fell below 1% of the peak value. To determine, in a comparable way, the duration of the high-frequency motor bursts in cells with an unclipped discharge pattern ($n = 12$), we first estimated the end of their high-frequency burst in the averaged control data by looking at the transition point between the high- and low-frequency discharge (see Fig. 6 for an illustration). The ratio between the peak spike-density and the spike density at the end of the burst, thus derived from the averaged control data, was subsequently used to detect the duration of each individual burst (for the different neurons, actual cutoff values ranged between 10 and 30% of the peak discharge rate). The latter was done by a computer algorithm that computed spike density functions with a σ of 10 ms (see METHODS). Because of the reduced firing rates during perturbed saccades (see e.g., Figs. 2 and 3; see also the quantitative data in following text), this relatively wide kernel was needed to obtain a more robust detection in both the perturbed and unperturbed condition (same σ used in both conditions and for all neurons). Although this procedure tends to overestimate the absolute duration of individual bursts (depending on the actual cutoff value), this overestimate is virtually fixed (within ~5 ms) across trials. It therefore has a negligible influence on the slopes and correlations of the linear regression analysis reported in the following text.

Figure 6, *top* and *bottom*, illustrates the results of this analysis for two different SRBNs. In Fig. 6, *A* and *C*, the burst duration is plotted versus eye-movement duration for all saccades around the respective movement field optimum. The data show that the duration of the motor burst of both cells correlated well with the actual saccade duration ($r = 0.85$ and $r = 0.65$ in Fig. 6, *A* and *C*, respectively; pooled conditions). As indicated in Fig. 6*B*, a 1% detection level could be used to measure the burst duration of *cell pj6701* since its discharge ended quite abruptly near the end of control saccades (i.e., clipped discharge). *Neuron er0904*, however, showed a buildup of prelude activity and a gradual decline of postsaccadic activity (i.e., unclipped discharge). As illustrated for the control condition in Fig. 6*D*, the end of its burst discharge was therefore taken at 30% of the peak discharge. Defined in this way, it appeared that the correlation between saccade and burst duration was much more comparable for the two cells than could be simply inferred from the spike density waveforms obtained in the control condition. Based on control saccades only, the relation between saccade and burst duration appeared to be less strict, as may be observed particularly for control responses obtained from *neuron er0904*. Note, however, that this apparent lack of correlation is mainly due to the substantial amount of intrinsic noise in the cell's responses (see also Sparks and Mays 1980) combined with the stereotyped nature of the control saccades. Indeed when only the perturbed responses (filled circle) in Fig. 6*C* were considered, a high correlation between saccade and burst duration was obtained also for this neuron ($r = 0.87$).

The histograms in Fig. 7 present a quantitative summary of the results for all 25 neurons analyzed in this way. Figure 7*A* shows the range of correlation values (pooled conditions). Note that the burst duration correlated well with the actual saccade duration in the majority of SRBNs; i.e., 20 neurons showed a

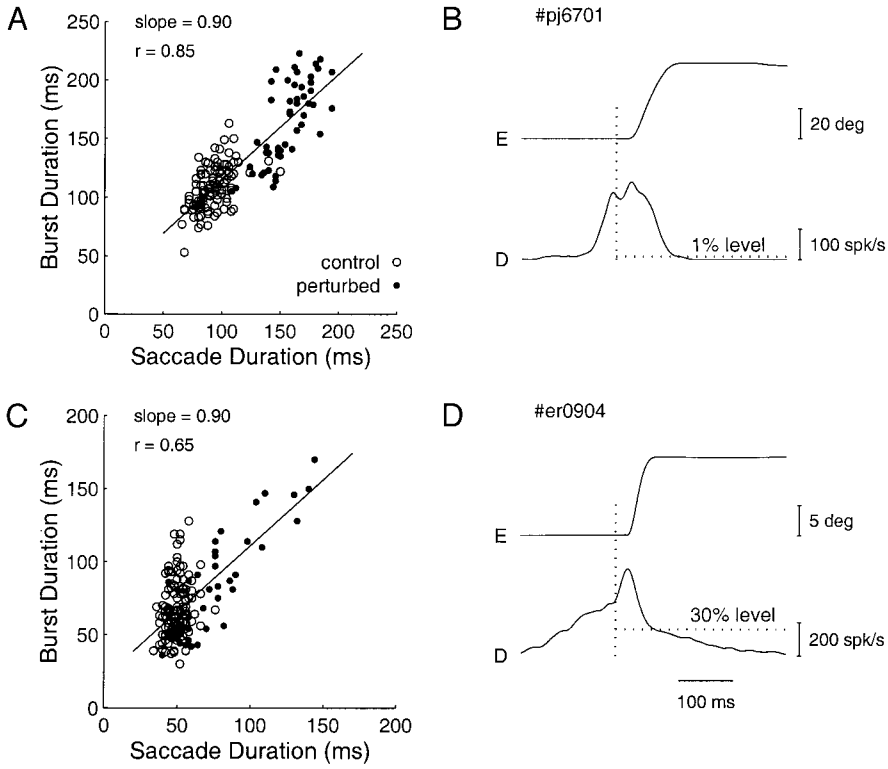

FIG. 6. Duration of the motor burst vs. saccade duration for 2 different SRBNs. *A* and *B*: burst duration of an SRBN (*pj6701*) that showed a clipped discharge. Data points in *A* scatter closely around a regression line with a slope of 0.90, indicating that the end of the motor burst in control trials (open circle) and perturbation trials (filled circle) was tightly coupled to saccade offset. As indicated in *B*, burst duration was measured from 20 ms before the saccade onset (vertical dotted line) to 1% of the peak discharge (horizontal dotted line; "1% level"). Plotted are the averaged radial eye position (*E*) and the spike-density waveform (*D;* σ = 10 ms) of a series of control saccades corresponding to the neuron's optimum vector ([*R*, Φ] = [50, 0] deg). *C* and *D*: comparable data for the high-frequency burst of an SRBN (*er0904*) that showed long-lead presaccadic activity. Note the buildup of prelude activity and the gradual decline of postsaccadic activity after the burst. Burst offset was taken at 30% of the peak discharge ("30% level"), where the mean spike-density waveform showed an inflection. Also for this neuron (optimum at [*R*, Φ] = [12, 180] deg), a significant relation between saccade duration and burst duration was obtained. This was most evident from the cell's responses in the perturbed condition (filled circle; correlation coefficient r = 0.87; slope = 1.13). Slopes and correlations indicated in *A* and *C* are based on pooled data from the 2 conditions.

significant correlation of $\geq$0.4 ($P < 0.001$). Low correlation values ($<$0.2) were obtained for five neurons. Since the saccade-related response of these latter neurons consisted of a weak burst discharge that contained only a few spikes, it may not be surprising that the activity measured during individual responses showed no significant correlation with saccade duration ($P > 0.1$). Indeed the strength of the correlation between saccade duration and burst duration appeared to be related to the average mean firing rate of the cells measured for control saccades of optimal amplitude and direction ($r = 0.56$, $P < 0.001$; not illustrated). Figure 7*B* shows the range of slopes obtained by fitting regression lines to the data of each particular cell (see Fig. 6). It may be observed that a wide range of slopes (0.0–0.98) was obtained and that the skewed distribution has its median ~0.7. Like the correlation values, the slopes also appeared to be related to the mean firing rate for optimal control saccades ($r = 0.51$, $P < 0.01$; not shown). It was verified that the results shown in Fig. 7 did not critically depend on the precise cutoff values used to detect burst offsets.

BURST MAGNITUDE. The raw data in Figs. 1–3 illustrate that the discharge rates were substantially lower during blink-perturbed saccades. However, the impression was obtained that the number of spikes in the motor burst was approximately similar for perturbed and control saccades. To better quantify this property, we counted the number of spikes in each burst for saccades of optimal amplitude and direction using a time window that ranged from 20 ms before saccade onset to saccade offset. For comparison, the total number of spikes before, during, and after the saccade also were quantified by counting all spikes over a fixed 800-ms window starting 100 ms after target onset (which excluded visually evoked activity). Perturbation trials in which the saccade kinematics appeared to be hardly affected were excluded from this analysis (typically <5–10% of the trials).

Figure 8 illustrates the results of this analysis for the two neurons shown in Fig. 6. Plotted are histograms of the number of spikes in the burst and the total number of spikes on individual control trials (*top*) and perturbation trials (*bottom*). Although the average number of spikes in the burst was slightly higher for perturbed saccades (*t*-test, $P < 0.01$), the difference between the two conditions was remarkably small. This result was obtained for *both* neurons (Fig. 8, *A* and *B*, and *E* and *F*), even though the number of spikes in the burst of the long-lead SRBN (*er0904*) was only a limited fraction of its total number of spikes (compare Fig. 8, *E* and *F* with *G* and *H*). The latter readily indicates that the long-lead SRBN also showed a considerable amount of pre- and postsaccadic activity (see also Fig. 6*D*). Note, however, that the total number of spikes for control responses and perturbed responses in the 800-ms window was very similar too (Fig. 8, *G* and *H*). For the short-lead SRBN (*pj6701*), the number of spikes in the burst and the total number of spikes was very similar (compare Fig. 8, *A* and *B* with *C* and *D*), which is readily understood from the clipped nature of its discharge (see also Fig. 6*B* and DISCUSSION).

The scatter plots in Fig. 9 summarize the quantitative results for all 25 fully tested SRBNs. The data in Fig. 9*A* show that, on average, the mean number of action potentials during perturbed saccades increased slightly with respect to the control condition. As a result, the linear regression line had a slope of 1.14 and a correlation coefficient of 0.94. Yet in view of the considerable spatial-temporal disturbances, the number of spikes

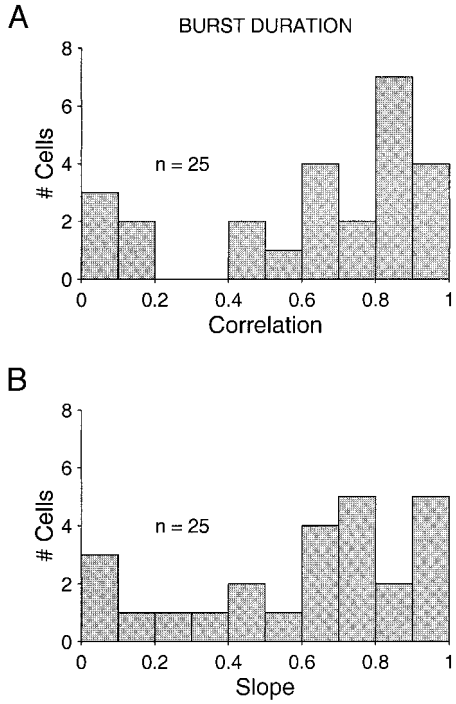

FIG. 7. Quantitative summary of the relationship between saccade and burst duration in the sample of 25 collicular neurons recorded in 3 monkeys. Slopes and correlations are based on pooled data from control trials and perturbation trials (typically, $n > 50$) and are pooled for the different SRBN subtypes. *A*: intermediate to high correlations were obtained for the majority of neurons ($n = 20$; $r > 0.4$; $P < 0.001$). No significant correlation was obtained for 5 cells ($r < 0.2$; $P > 0.1$). *B*: range of slopes obtained by fitting linear regression lines to the data (see Fig. 6). Slopes tend to cluster around 0.7–0.8.

for perturbed saccades was remarkably similar to the number of spikes in the burst for control movements. Indeed the apparent increase was not significant (*t*-test, $P > 0.1$) in about half of the cells ($n = 15$) and did not reach the 1% criterion in another three neurons. Since blink-evoked perturbations typically resulted in much longer saccade durations, the mean firing rate was substantially reduced in the perturbed condition. This is further quantified in Fig. 9*B*. Note that the slope of the regression line is now only 0.48, indicating a significant reduction in the mean firing rate across the recorded SRBNs (*t*-test, $P < 0.01$ for 17 cells). Similar results were obtained for movements of less optimal amplitude and direction (data not shown).

When the number of spikes in the burst is fixed and burst duration correlates with saccade duration, it may be expected that the mean firing rate in the burst is related to the mean saccade velocity (defined as amplitude/duration). This feature is exemplified in Fig. 10, *A* and *B*, which shows this relation for the two cells also illustrated in Figs. 6 and 8. Note that there was a significant ($P < 0.01$) correlation for both cells ($r = 0.54$ and $r = 0.49$ in *A* and *B*, respectively). Figure 10, *C* and *D*, summarizes the correlation coefficients and slopes of the linear regression lines, respectively, for the whole population of 25 fully tested cells. The correlation was highly significant for the majority of cells ($P < 0.0001$ for $n = 13$ cells, and $0.0001 < P < 0.01$ for $n = 9$ cells), two cells did not reach the 1% criterion, and only one cell showed no significant correlation ($P > 0.1$). The population average of the correlation coefficients was 0.67 (range: 0.28–0.90; median: 0.72). The sensitivity of the cells, indicated by the slope values, varied substantially from cell to cell (range: 0.04–1.68 spikes/s per °/s; median: 0.28 spikes/s per °/s) and depended on a cell's average mean firing rate ($r = -0.42$, $P < 0.04$; cf., Fig. 10, *A* and *B*).

The data presented so far demonstrate that the temporal characteristics of the SC activity during blink-perturbed saccades were considerably modified with respect to the control condition. In summary, we found a transient decrease in SRBN activity around the onset of a blink as well as a subsequent prolongation of the SRBN discharge in line with the increase in saccade duration. Moreover the mean firing rate was reduced during perturbed saccades in such a way that there were an approximately equal number of spikes in the burst as for control saccades. These findings therefore show that blinking interferes with saccade generation at the level of the midbrain SC.

Intrasaccadic discharge in relation to the 2-D saccade trajectory

The observed linkage between saccade duration and burst duration (Figs. 6 and 7) could be expected if the SC is part of the local feedback loop that is thought to control the saccade trajectory (see INTRODUCTION). To further investigate this possibility, we therefore analyzed the intrasaccadic discharge of collicular neurons in relation to the *2-D* saccade trajectory.

SPATIAL PROPERTIES. Figure 11 shows a typical example of the results of this analysis for an SRBN that was most active for upward control saccades (movement field center $[R, \Phi] \approx [35, 90]$ deg). Figure 11, *A–C*, shows the 2-D trajectories of a perturbed saccade and a control saccade toward the same target (Fig. 11*A*; T at $[R, \Phi] = [27, 60]$ deg) as well as simultaneous records of the cell's discharge during each of these movements (Fig. 11, *B* and *C*, respectively). Figure 11, *D–F*, shows data of two visually evoked control saccades that matched to the two subsequent eye-movement phases that were present in the perturbed saccade. Comparing the perturbed response in Fig. 11*B* to the control response in Fig. 11*C*, one may observe that the duration of the saccade-related discharge during the perturbed response exceeded the normal burst duration by far. The most important feature, however, is that the cell resumed its burst activity after the blink-related suppression even though the *direction* of the compensatory movement (rightward) did *not* match the *direction* of the cell's movement field (upward). The latter becomes evident by noting that the compensatory movement in Fig. 11*B* was almost equivalent (albeit slower) to the rightward saccade plotted in Fig. 11*E* (cf., Fig. 11, *A* and *D*) and by noting that the cell was not at all recruited for this control saccade. Because the neuron resumed its burst activity, we conclude that the compensatory movement was still part of the initial saccade program specifying an eye displacement up and to the right. If the compensatory movement had instead been generated by a new motor command specifying a rightward eye displacement, the discharge of the neuron should have stopped completely when the eye moved rightward (see Fig. 11*E*). Note that these results closely resemble the results obtained in the interruption paradigms used previously (see INTRODUCTION) except that in this case the direction of the compensatory movement has been altered too. The initial phase of the perturbed response is also quite interesting. In this part of the response, the eye movement was directed *into* the

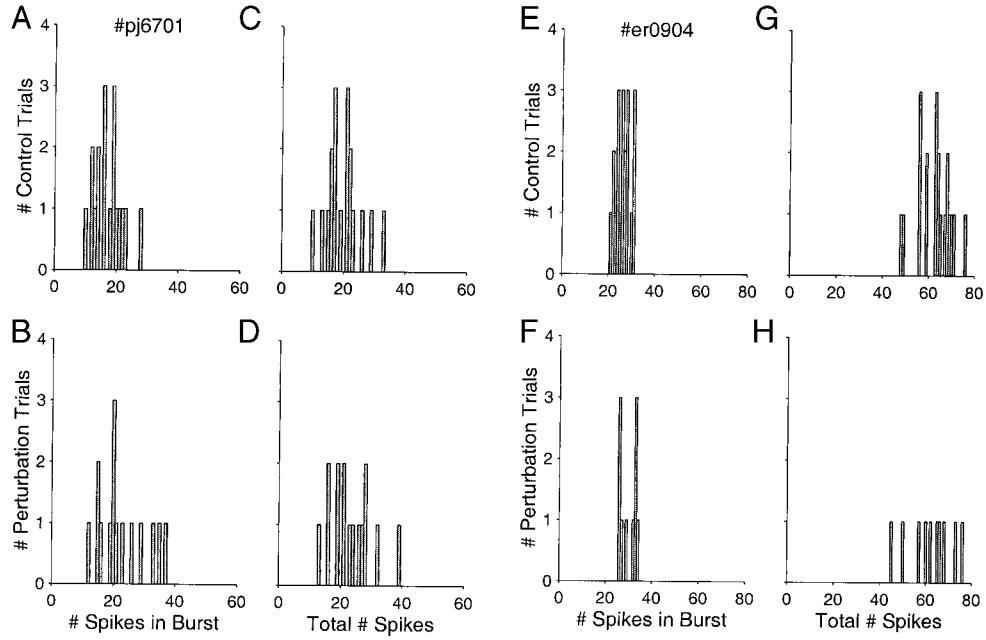

FIG. 8. Similar number of spikes in the burst for control and perturbed saccades toward the movement field center illustrated for 2 different SRBNs. The burst was taken from 20 ms before saccade onset until saccade offset. The total number of spikes before, during, and after the saccade was quantified over a fixed period of 800 ms starting 100 ms after target onset. *A–D*: data obtained from a clipped SRBN showing little prelude activity (*pj6701*). Same neuron as in Fig. 6, *A* and *B*. Histograms *A* and *B* show the number of spikes in the burst for control and perturbed saccades of optimal amplitude and direction. Histograms *C* and *D* show the total number of spikes in the same trials (800-ms window). The average number of spikes in the burst was 17 ± 5 (mean ± SD; $n = 18$) and 23 ± 8 ($n = 15$) in *A* and *B*, respectively. The average total number of spikes in *C* and *D* was 19 ± 6 and 23 ± 6, respectively. *E–H*: similar data from an unclipped cell showing long-lead presaccadic activity (*er0904*). Same neuron as in Fig. 6, *C* and *D*. The average number of spikes in the burst was 26 ± 3 ($n = 20$) and 30 ± 3 ($n = 10$) in *E* and *F*, respectively. The average total number of spikes in *G* and *H* was 63 ± 7 and 62 ± 9, respectively. Note that the number of spikes in the burst for control saccades and perturbed saccades was very similar for both neurons. Note also that the total number of spikes appeared to be similar too and that the number of spikes in the burst was only a small fraction of the total number of spikes for the neuron shown in *E–H*.

cell's movement field (upward). As may be observed in Fig. 11, *A* and *D*, the amplitude and direction of this initial movement were comparable with that of the upward control saccade. Note, however, that during the upward movement in Fig. 11*B*, the cell showed a near-complete cessation of activity (see first 50–60 ms), whereas the cell discharged vigorously for the upward control saccade plotted in Fig. 11*F*. Because the SRBN showed a near-complete cessation of activity even though the eye moved in the optimal direction of the cell, we conclude that the SRBN discharge did not mediate the upward trajectory perturbation. If the upward movement had instead been generated a (modified) collicular command specifying an upward eye displacement, the cell should have continued its vigorous discharge during the upward movement (see Fig. 11*F*). Summarizing these results, it appears that the actual 2-D trajectory of the perturbed saccade was not reflected in the SRBN discharge pattern.

DISCHARGE DYNAMICS. For all neurons that could be tested in detail, phase plots were constructed of instantaneous spike density versus radial motor error (*ME;* difference between desired and current eye displacement) by following the same method utilized in previous studies (Keller and Edelman 1994; Munoz et al. 1996; Waitzman et al. 1991). The majority of these cells ($n = 17$) showed a monotonic decline of spike density as function of decreasing radial motor error for control saccades toward the center of their movement field and were therefore subjected to a further analysis. Since blinks not only modified the saccade kinematics but also changed the 2-D saccade trajectories, additional phase plots were made of spike density versus the respective horizontal and vertical motor-error components. Spike density functions were computed with a σ of 4 ms and shifted backward in time by 4–8 ms to obtain the best linear decline as function of radial motor error for control responses (Waitzman et al. 1991).

Typical results of this type of analysis are illustrated in Fig. 12 for one of the recorded SRBNs. Saccades were evoked toward targets at $[R, \Phi] = [14, 60]$ deg, which corresponded closely to the movement field optimum of the cell. As in Fig. 11, the instantaneous movement direction of the eye during the compensatory phase fell outside the neuron's movement field (right and upward; not indicated) and was approximately orthogonal to the movement direction during control saccades (see Fig. 12*A*). The neuron's prolonged motor burst for perturbed saccades is depicted in Fig. 12*B*. The phase plots in Fig. 12, *C–E*, show spike density as function of radial, horizontal, and vertical motor-error components, respectively. Note that the intrasaccadic decline of spike density during control saccades (averaged data only; thin solid curves) was nearly linearly related to the decrease in *each* motor error component. The latter results, of course, from the fact that the control saccades were approximately straight (see Fig. 12*A*). For perturbed saccades (averaged data: thick solid curves*;* individual responses: dots at 2-ms time resolution), however, clearly different curves were obtained that were no longer monotonic.

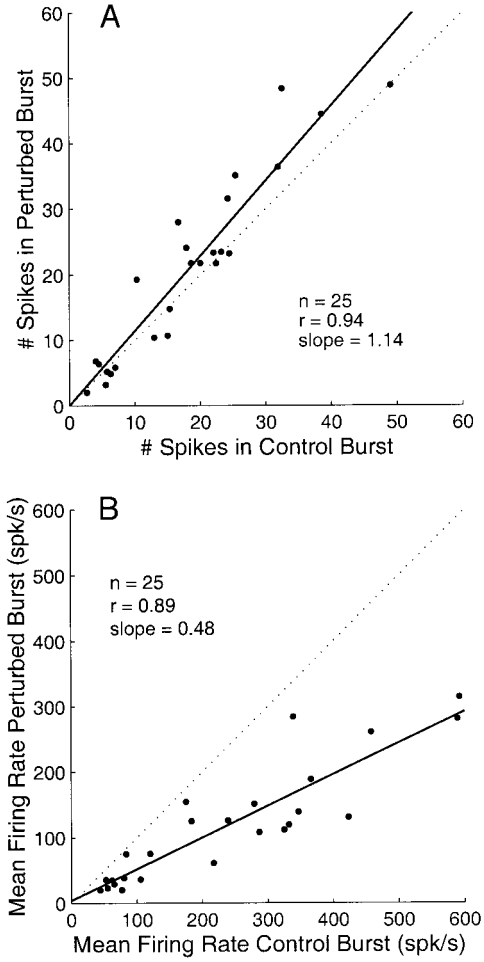

FIG. 9. Number of spikes in the burst and mean firing rate in the burst for control and perturbed saccades of optimal amplitude and direction for all 25 fully tested cells. *A*: the average number of spikes in the burst showed relatively little change even though the spatial-temporal properties of the saccades were always substantially modified. In most neurons, the number of spikes in the burst increased only slightly ($P < 0.01$ for $n = 7$ cells; $P > 0.1$ for $n = 15$ cells), resulting in a slope of 1.14 of the regression line. Average spike counts were typically based on ≥10 trials, and in no case were <5 trials used. *B*: a significant reduction of the mean firing rate in the burst was obtained for most cells ($n = 17$; $P < 0.01$), resulting in a slope of only 0.48 of the overall regression line. This is readily understood from the fact that comparable spike counts were obtained for movements of much longer durations.

At the onset of perturbed movements (i.e., at the largest *ME* values), spike density fell significantly below the control curves. Interestingly, the relation of spike density with radial and horizontal motor-error (Fig. 12, *C* and *D*) became, on average, comparable with the control relation near the end of the movement (i.e., at *ME* values below ~5°). One may realize, however, that the actual 2-D saccade trajectories were considerably different during this compensatory phase (see Fig. 12*A*). Hence it appeared that the neuron showed a comparable instantaneous discharge but for quite different eye movements. The latter is underlined by Fig. 12*E*, which shows that the relation of spike density with vertical motor error was very different from the control curve throughout the perturbed movement. As can be noticed in Fig. 12, *A* and *B*, this results from the fact that vertical motor error did not change monotonically as function of time.

Figure 13 demonstrates the reproducibility of these findings among the 17 neurons analyzed in this way. The plots in Fig. 13, *A–C* and *D–F*, show the results obtained from two other SRBNs whose temporal discharge patterns are shown in Figs. 2 and 3, respectively. Although these SRBNs were endowed with quite different pre- and postsaccadic discharge properties, the three plots of intrasaccadic spike density versus dynamic motor error were qualitatively similar for the two neurons. In both cases, the final portion of the phase curves tends to coincide for radial and horizontal motor error components. Yet because of the highly curved nature of the saccade trajectories (see also Goossens and Van Opstal 2000), spike density versus vertical motor error yielded nonmonotonic relations also at the end of the perturbed movements.

Figure 13*G* shows the average normalized behavior of all 17 neurons during control saccades (population average only; thick dashed curve) and during perturbed saccades (population average: thick solid curve; individual neurons: thin solid curves). Note that the phase relations are clearly different for the two conditions. Only three neurons showed a more or less similar relation for two conditions, but in those recording sessions, the actual perturbations were relatively small. A direct comparison between the average control and perturbed response of each individual neuron is provided in Fig. 13*H*. In this figure, the average normalized activity during control saccades is plotted against the averaged normalized activity during perturbed saccades (thin curves) for corresponding ME values. The population average is superimposed (thick curve). Both radial motor error and time are implicit in this plot. Note that there are large deviations from the identity line (dashed), indicating that there was no consistent relation between spike density and dynamic motor error in the far majority of cells.

Activity during saccades showing no compensation

So far we have presented an analysis of the SRBN discharge properties during saccades that compensated for the blink-related perturbations. Typically the SC cells remained active throughout these movements, irrespective of the instantaneous eye-movement trajectory. It is therefore of interest to also consider what happened in cases where compensation was absent (see also Goossens and Van Opstal 2000). Although this latter response mode was quite uncommon (usually no more than 15% of the trials), it was typically found in those cases that the cell stopped firing well before the eye-movement offset. Examples of this behavior are shown in Fig. 14.

Figure 14*A* depicts the 2-D trajectories of four blink-perturbed saccades (· · · ; mean indicated by —) that showed compensation for the disturbance (mainly in velocity). The cell's prolonged burst discharge until the end of these saccades into its movement field (center at $[R, \Phi] = [40, 200]$ deg) is plotted in Fig. 14*B*. Figure 14, *C* and *D*, shows the data obtained in five perturbation trials where no compensation occurred. Rather after the initial movement toward the target, the eye started moving upward, a direction that was not into the cell's movement field (leftward; not indicated). It can be clearly observed that in these cases the cell's initial burst discharge stopped as soon as the eye stopped moving toward the target.

These observations raised the question what would happen in the converse case when a nongoal-directed movement would be made into a cell's movement field. We therefore attempted

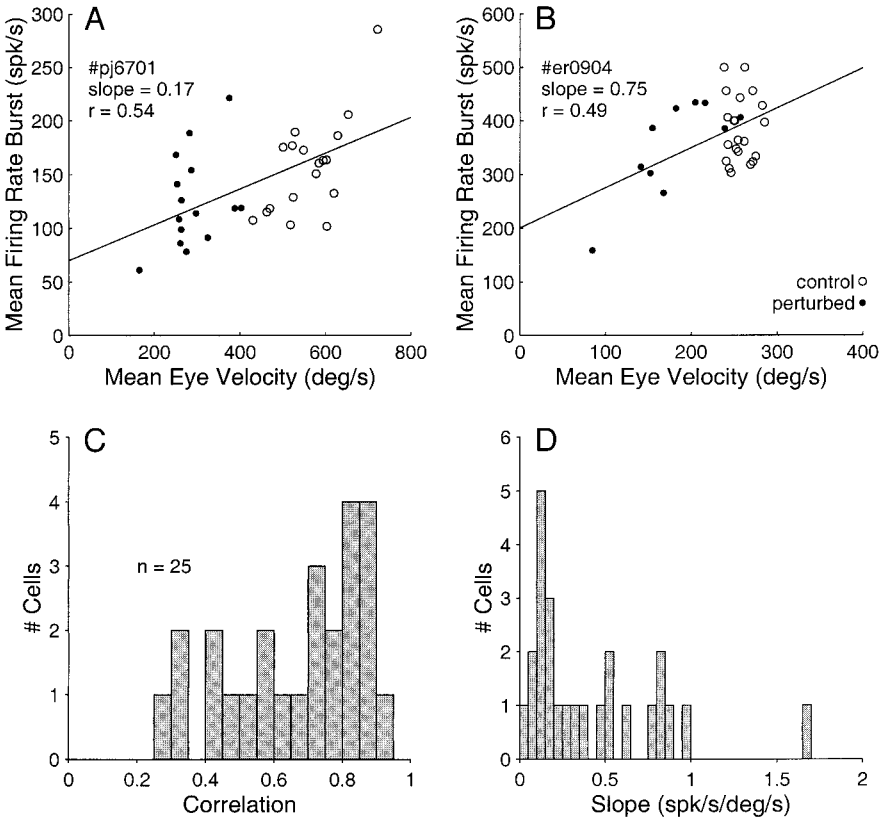

FIG. 10. Mean firing rate in the motor burst is correlated with mean eye velocity. *A*: results for individual responses in control (○) and perturbation (●) trials of *cell pj6701* (burst type). *B*: same analysis for cell *er0904* (buildup type). *C*: summary of the correlation coefficients obtained for all 25 fully tested cells. For the far majority of cells (22/25), the correlation was significant ($P < 0.01$). Population average was 0.67 (median: 0.72; range: 0.28–0.90). *D*: slopes of the regression lines for all 25 neurons vary substantially from cell to cell, although clustering occurs between 0.0 and 0.25 (median: 0.28 spikes/s per °/s; range: 0.04–1.68 spikes/s per °/s).

to elicit such eye movements in the direction of the preferred vector of several neurons studied, but sufficient data could be obtained in only three recording sessions. It is nevertheless interesting to consider the results of this particular experiment, which is illustrated in Fig. 15 for one of these neurons. Figure 15*A* depicts blink-perturbed saccades toward target T1, which was flashed on the horizontal meridian. Note that all movements were goal-directed and showed compensation for the blink-related perturbation. Despite the disturbances, the neuron (*er1101*) showed a brisk discharge during these movements, which were directed into the movement field (optimum at [R, Φ] = [14, 150] deg). Figure 15*B* shows the cell's response during a series of control saccades made outside its movement field. As one may readily infer from this figure, the neuron was completely silent during these movements. Figure 15*C* shows blink-perturbed eye movements that were obtained while the animal was required to make saccades toward T2, but no compensation occurred. Luckily the resulting eye movements in these particular trials were directed into the cell's movement field, and they were also quite comparable to the ones shown in Fig. 15*A*. Note, however, that the cell's burst discharge remained absent (Fig. 15*C*). The two other SRBNs showed a similar behavior. These data therefore support the idea that SRBNs are recruited only for planned movements into their movement fields.

DISCUSSION

In the present experiments, we have investigated the influence of blinking on the saccade-related discharge patterns in the intermediate and deep layers of the SC. The results demonstrate, for the first time, that trigeminal reflex blinks have a profound influence on the saccade-related discharge of collicular SRBNs. In summary, it was found that ~10 ms after the air puff reached the eye, SRBN activity was briefly suppressed, ~10 ms before the onset of the evoked blink reflex; all recorded SRBNs resumed their discharge shortly (10–30 ms) after the blink onset; all SRBNs continued their discharge for goal-directed saccades into their movement field, irrespective of the saccade duration and irrespective of the instantaneous eye-movement direction; the duration of the high-frequency burst was approximately matched to the overall saccade duration for the majority of cells, regardless of their pre- and postsaccadic discharge properties; although the saccade kinematics and trajectories were both profoundly affected and variable, the number of spikes in the burst was remarkably similar for control and perturbed movements, whereas the mean firing rate was strongly reduced (~50%); for most cells, mean firing rate in the burst and mean eye velocity were well correlated; the monotonic relation between spike density and dynamic motor error, often observed for control saccades, broke down for perturbed saccades; large changes in instantaneous eye-movement direction were not reflected in the instantaneous discharge rate of SRBNs; SRBN activity stopped prematurely when saccades showed no compensation; and finally SRBNs remained silent when eye movements made into the cells' movement field were not part of a planned movement.

Taken together, the data presented in this paper and in the companion paper (Goossens and Van Opstal 2000) show that reflex blinks change many parameters: saccade latency, eye velocity, saccade duration, and saccade trajectories as well as SRBN firing rates and SRBN burst duration. The only two

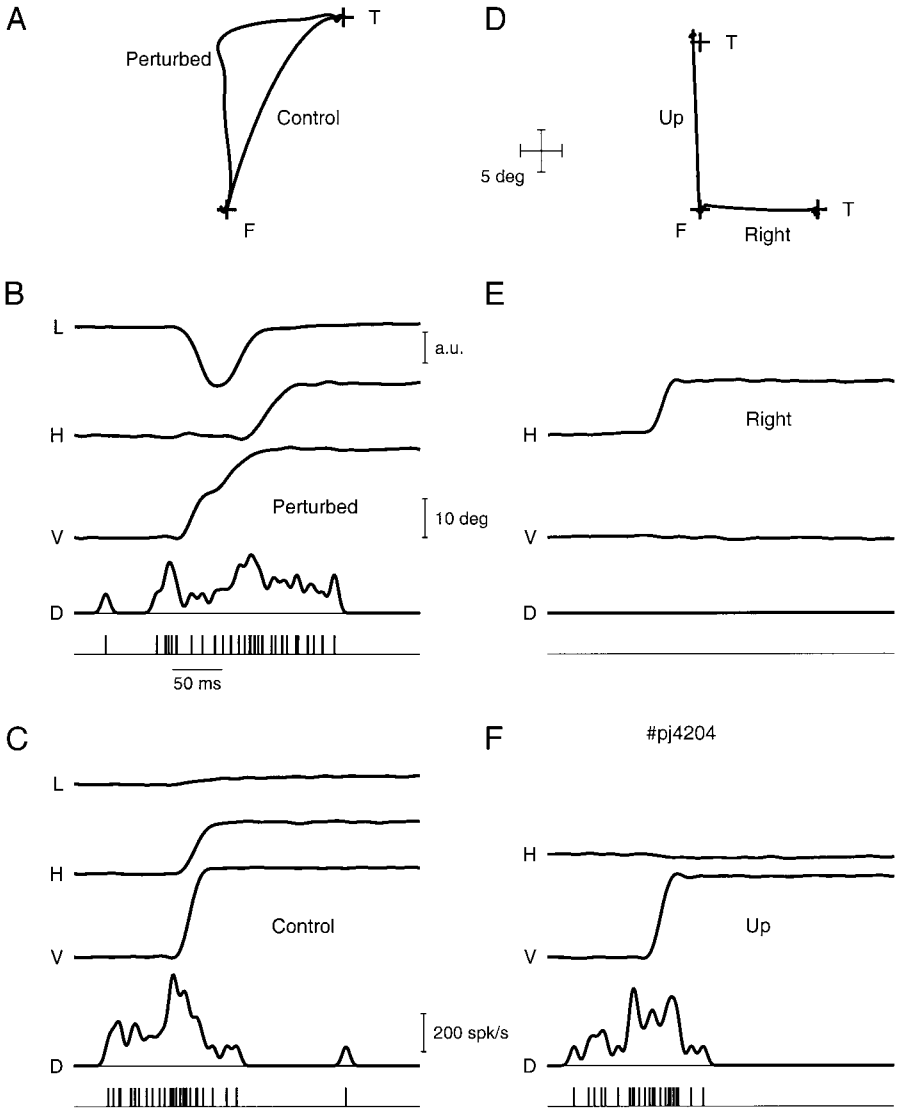

FIG. 11. SRBNs resumed their burst activity irrespective of the instantaneous eye-movement direction. Example from *neuron pj4204*. *A*: 2-dimensional (2-D) trajectories of a *control* saccade and a *perturbed* saccade of equal amplitude and direction evoked from the fixation point (*F*) toward a briefly flashed visual target (*T*, presented at [*R*, Φ]] = [27, 60]). The movement field optimum was at [*R*, Φ] ≈ [35, 90]. *B* and *C*: plots of eyelid (*L*, vertical) and eye (*H*, horizontal; *V*, vertical) position as function of time for the 2 movements shown in *A*. Simultaneous records of the neuron's activity are plotted underneath. Shown are the spike density functions (*D;* σ = 4 ms) and individual action potentials (vertical lines). *D–F*: similar data for an *upward* and a *rightward* control saccade matched, respectively, to the initial upward and subsequent rightward eye-movement phase of the perturbed saccade shown in *A* and *B*. Note that the burst activity of the cell was transiently suppressed (see 1st 50–60 after saccade onset in *B*) even though the perturbed saccade consisted of an initial upward movement that was directed *into* the cell's movement field (see burst in *F*). Note also that the neuron subsequently resumed its burst discharge until the eye had reached the target (see *B*) despite the increase in movement duration with respect to the control saccade in *C* and despite the fact that the rightward, compensatory movement fell *outside* the cell's movement field (see absence of activity in *E*).

variables that remained virtually unaffected were the overall saccade displacement vectors and the number of spikes in the burst. Our findings therefore strongly suggest that the number of spikes in the burst of collicular SRBNs specify the desired displacement vector of the eye rather than its actual 2-D trajectory. The data also indicate that the observed perturbations of the saccade trajectories are compensated by mechanisms that act downstream from the motor SC rather than by local feedback through the SC. This hypothesis will be discussed in the subsequent sections.

Saccade-blink interactions

Previous experiments have shown that trigeminal reflex blinks are suppressed by excitation of the SC presumably because the SC excites a nonsaccadic pathway that inhibits the reflex blink circuitry (Basso and Evinger 1996; Basso et al. 1996; Gnadt et al. 1997). The results of the present study show that reflex blinks (or blink-evoking air puff stimuli), in turn, inhibit saccade-related activity of the SC. Thus the picture of an antagonist interaction between the saccade and blink systems emerges.

Nevertheless, (large) saccades tend to be accompanied by blinks (Evinger et al. 1991; Zee et al. 1983), the gaze-evoked blinks, which may result from a linkage between the saccadic and blink systems (Evinger et al. 1994). Furthermore despite the suppressive effect on SRBN activity, air-puff-evoked blinks yielded *reduced* saccade latencies (see Goossens and Van Opstal 2000). Presumably, this effect results, at least in part, from saccade-blink interactions at a different level in the premotor circuitry. It has been shown that blinks are accompanied by a pause in the tonic OPN discharge (Cohen and Henn 1972; Fuchs et al. 1991; Mays and Morrisse 1994). As a result, the reduced firing rates of collicular SRBNs (Fig. 9*B*) can still gain access to the saccadic burst generator, which is otherwise inhibited by the OPNs. Apparently, these low collicular activation levels also result in much slower saccades (e.g., Figs. 2 and 3 and 10) (see also Berthoz et al. 1986; Van Opstal and Van Gisbergen 1990).

Suppression of SRBN discharge

An interesting feature that was observed in most of the recorded SRBNs was a brief suppression of their discharge

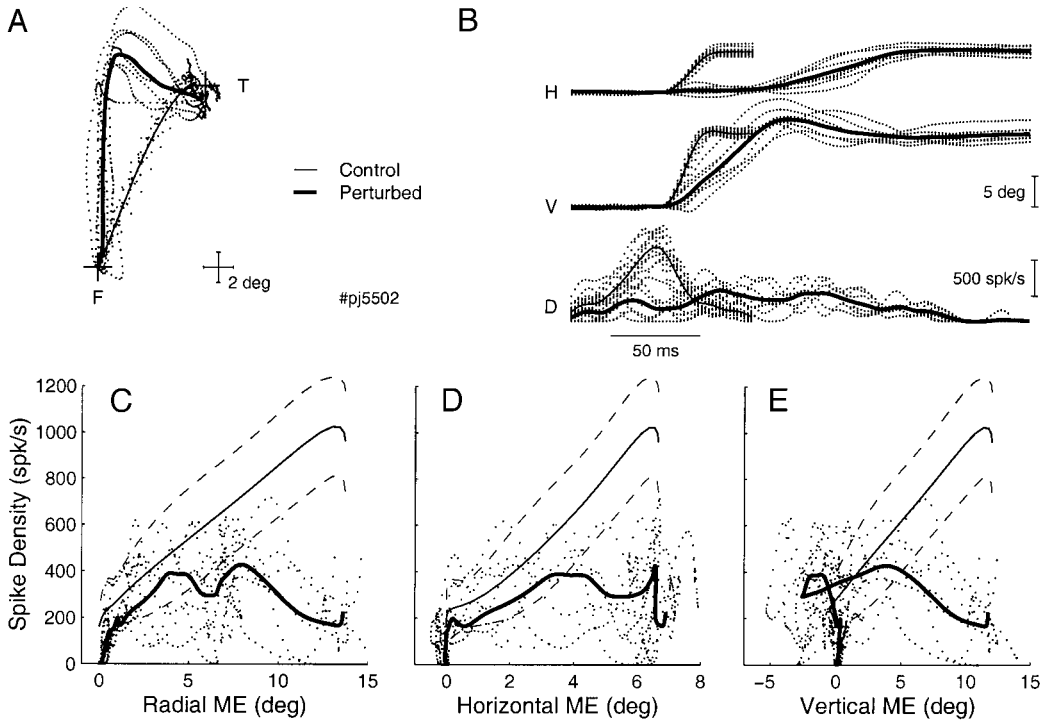

FIG. 12. Typical discharge dynamics in relation to the 2-D trajectories of visually evoked saccades, illustrated for 1 of the recorded SRBNs (*pj5501*). *A*: 2-D trajectories of a series of control saccades and blink-perturbed saccades toward targets flashed at [*R*, Φ] = [14, 60]. Amplitude and direction of the saccade vectors closely matched the cells' optimum vector, but the compensatory movement during perturbed saccades was approximately orthogonal to the control trajectories. *B*: spike density functions (*D;* σ = 4 ms) and horizontal (*H*) and vertical (*V*) eye position components as function of time. Control movements and spike density functions are cutoff for clarity. Note sustained discharge during perturbed saccades until eye-movement offset even though the compensatory movements were made *outside* the cell's movement field (right and upward; not indicated). *C–E*: phase plots of spike density versus radial, horizontal, and vertical dynamic motor error (*ME*) components, respectively. Dynamic motor error is the difference between saccade endpoint and instantaneous eye position ($HME = H_t - H_{end}$; $VME = V_t - H_{end}$; $RME = \sqrt{HME^2 + VME^2}$). The curves begin at the largest motor error values and proceed, in a counterclockwise loop, toward 0. Time is implicit in these plots. The spike density functions were shifted backward in time by 7 ms to obtain the best linear decline as function of radial motor error for control saccades. Note scale differences. Each panel shows the sampled records of individual perturbed responses (dots at a time resolution of 2 ms). Solid lines show the averaged control responses (thin lines) and perturbed responses (thick lines). Dashed lines in *C–E* denote standard deviations of the averaged control curves. Note the monotonic, nearly linear, relation with *each* motor error component for control saccades. Also note quite different and complex, nonmonotonic curves in the case of perturbed movements. The final portion of these curves tends to coincide with the control curves in *C* and *D* but not in *E* due to the highly curved nature of the saccade trajectories (see also Goossens and Van Opstal 2000). Hence, the neuron showed a comparable activity near the end of the perturbed and control movements, even though the instantaneous eye-movement *direction* was distinctly different (see *A*).

following the onset of an air puff (Figs. 2–5). Also the mean firing rates were reduced considerably in the majority of cells (Fig. 9). Our experiments provide no direct evidence concerning the mechanisms underlying these phenomena.

TRIGEMINOTECTAL PATHWAY. One possibility is that the observed suppression is due to afferent input from principal sensory and spinal trigeminal neurons that innervate the SC (e.g., Huerta et al. 1981, 1983; Wiberg et al. 1987). This possibility is supported by our observation that SRBN activity was only mildly affected by gaze-evoked blink, whereas a strong suppression was observed during air-puff-evoked blinking in about one-third of the cells (Figs. 4 and 5). Also the latency of this effect, estimated at ~10 ms relative to air puff onset (Fig. 5), seems to be roughly in line with what could be expected for a trigiminotectal pathway in rhesus monkey. However, it is currently unknown whether the SRBNs in monkey receive *inhibitory* trigeminal signals, either directly or indirectly (via interneurons). Earlier work, by e.g. Redgrave et al. (1996), suggests that trigeminal afferents to the SC are *excitatory* because their study showed that SC neurons increase their discharge in relation to nociceptive and wide-dynamic-range facial stimuli in anesthetized rat. It is unclear, however, whether they recorded from movement-related cells analogous to SRBNs. In our present experiments, we obtained no evidence that SRBNs in the monkey SC are excited by trigeminal signals.

CEREBELLOTECTAL PATHWAY. An alternative possibility is that a cerebellotectal pathway mediates the suppression of SRBN activity. As reported by May et al. (1990), the monkey SC receives cerebellar input via two pathways. One, the fastigiotectal pathway, is derived from cells in the caudal fastigial nucleus that project bilaterally to the rostral SC. The other pathway is derived from cells in the interposed nucleus and the dentate nucleus, which project to the intermediate and deep layers of the contralateral SC. In cat, cerebellar dentate neurons are related to both saccade and eyelid parameters (Gruart and Delgado-García 1994). However, it remains to be determined whether dentate projec-

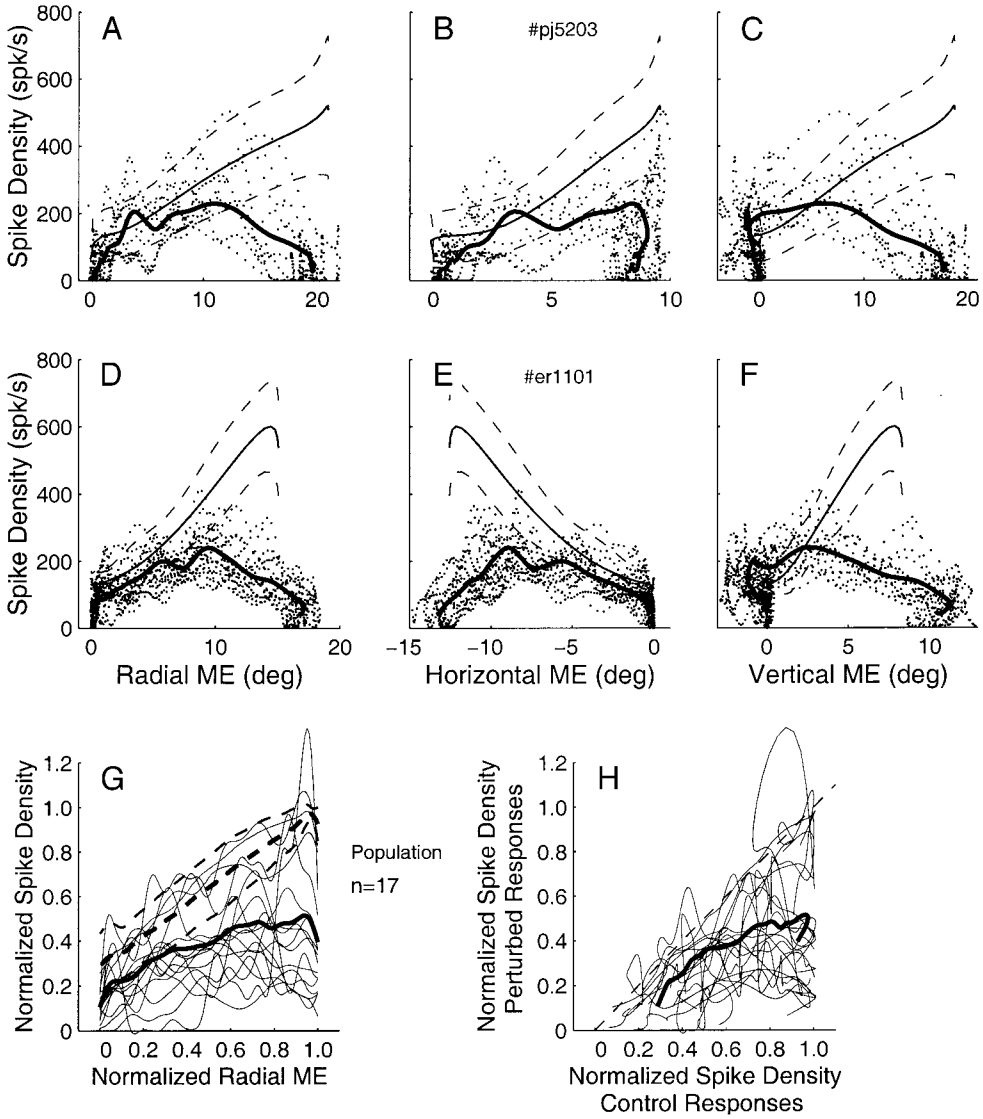

FIG. 13. Relation between instantaneous spike density and dynamic motor error was different under the 2 experimental conditions. *A–F*: phase plots of intrasaccadic spike density as function of dynamic motor error for 2 representative neurons endowed with different presaccadic and postsaccadic discharge properties. Same layout as Fig. 12, *C–E*. *A–C*: spike density of a clipped SRBN (*pj5203*) as function of dynamic motor error. The activity of this neuron as function of time is shown in Fig. 2 (same responses, except the 2 with a late perturbation). *D–F*: similar data for an unclipped SRBN (*er1101*) endowed with long-lead presaccadic activity. Figure 3 shows the temporal discharge pattern of this neuron during the same responses (except the 1 response with a late perturbation). Note clearly different phase curves for control saccades (thin curves) and perturbed saccades (thick curves) in all 6 panels but qualitatively similar results for the 2 SRBNs. *G*: normalized phase curves for the 17 neurons analyzed in this way. Dashed curves: mean (thick) and standard deviation (thin) of the pooled control data from all 17 neurons. Solid curves: averaged data from each individual neuron (thin) in the perturbed condition with the population mean (thick) superimposed. Spike density was resampled as function of radial motor error to account for variability in saccade kinematics (see METHODS). *H*: spike density during perturbed saccades vs. spike density during control saccades at the same radial ME for each individual neuron (thin curves) with the population mean (thick curve) superimposed. Radial motor error and time are both implicit. Note that virtually all curves are nonmonotonic and that there are considerable deviations from the identity line (dashed).

tions to the SC exert a short-latency, transient inhibitory influence on collicular SRBNs.

NIGROTECTAL PATHWAY. A third possibility is that the substantia nigra pars reticulata (SNr) of the basal ganglia is involved. As far as we know, only the SNr is currently known to have strong inhibitory projections throughout the motor SC (e.g., Beckstead et al. 1981; Graybiel 1978; May and Hall 1986). Many SNr cells normally decrease their tonic discharge before and during a saccade, thus allowing a brisk burst discharge by collicular SRBNs (Hikosaka and Wurtz 1983). Recent studies in rat have furthermore indicated that the amplitude of reflex blinks can be modulated through a nigro-tectal-spinal pathway (Basso and Evinger 1996; Basso et al. 1993, 1996; Evinger et al. 1993). Inactivation of the SNr by microinjections of muscimol, for example, yielded a suppression of reflex blinks in rats (Basso et al. 1996) as did electrical microstimulation of the SC in both rats and monkeys (Basso et al. 1996; Gnadt et al. 1997). Microinjections of muscimol into the rat SC, in turn, led to an enhancement of reflex blinks (Basso et al. 1996). In addition, neurological disorders like Parkinson's and Huntington's disease give rise to both marked oculomotor deficits, such as slow saccades, and an abnormal reflex blink excitability that may be partly due to a disturbed SNr input to the SC (Basso and Evinger 1996; Basso et al. 1996; Bronstein and Kennard 1985; Hikosaka and Wurtz 1983; Leigh et al. 1983; Rascol et al. 1989; White et al. 1989). Taken together, it is conceivable therefore that the SNr could be involved in modifying the SRBN discharge during blinks. Perhaps reflex blinks give rise to a transient excitation of SNr cells, causing a suppression of SRBN burst discharge. The latter, in turn, would facilitate reflex blinks at the time of a saccade. A similar hypothesis has been put forward by McHaffie et al. (1989), who proposed a model of competitive interactions between SC-mediated orienting and defensive reflexes, in which the orienting responses are suppressed by inhibition via the basal ganglia while withdrawal responses are initiated. However, it remains to be shown that blinks actually influence the activity of SNr cells.

INTRACOLLICULAR MECHANISMS. A transient suppression of SRBN activity also occurred when intrasaccadic microstimu-

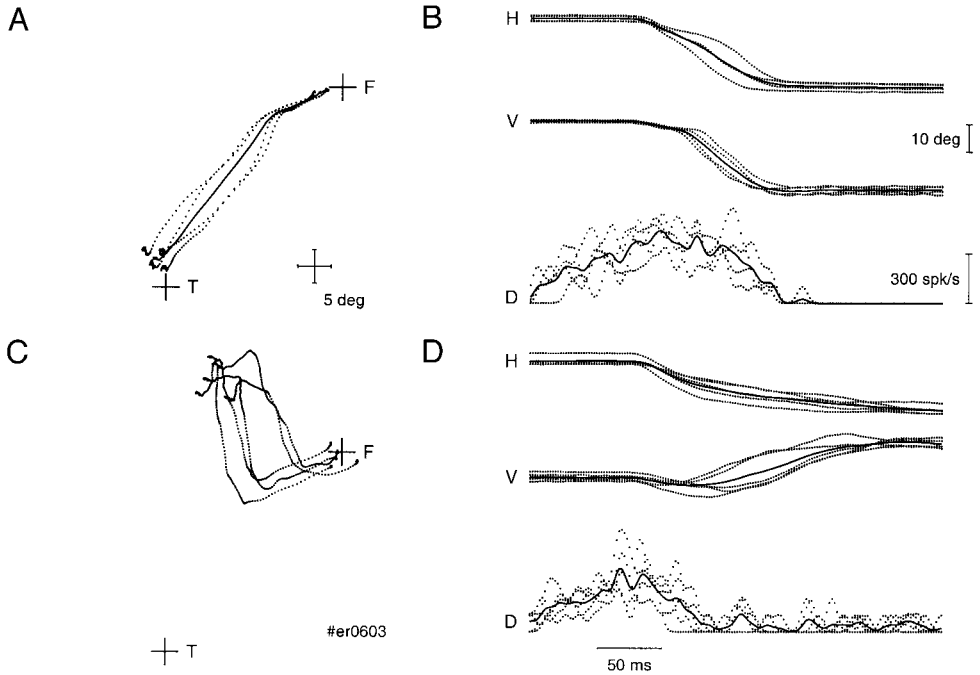

FIG. 14. The SRBN discharged stopped well before the end of the movement when there was no compensation for the blink-related perturbation. Data from *cell er0603*. *A* and *B*: spatial trajectories and eye-position traces (*H* and *V*) of blink-perturbed eye movements into the cell's movement field (optimum $[R, \Phi] \approx [40, 210]$ deg) exhibiting compensation. Spike density functions (*D*) show the synchronization of the neuron's discharge with saccade offset. *C* and *D*: similar data as in *A* and *B*, but now the saccades showed no compensation. Note that the burst discharge of the cell stopped when the eye started moving upward. The eye movements ended just outside of the neuron's movement field (not indicated).

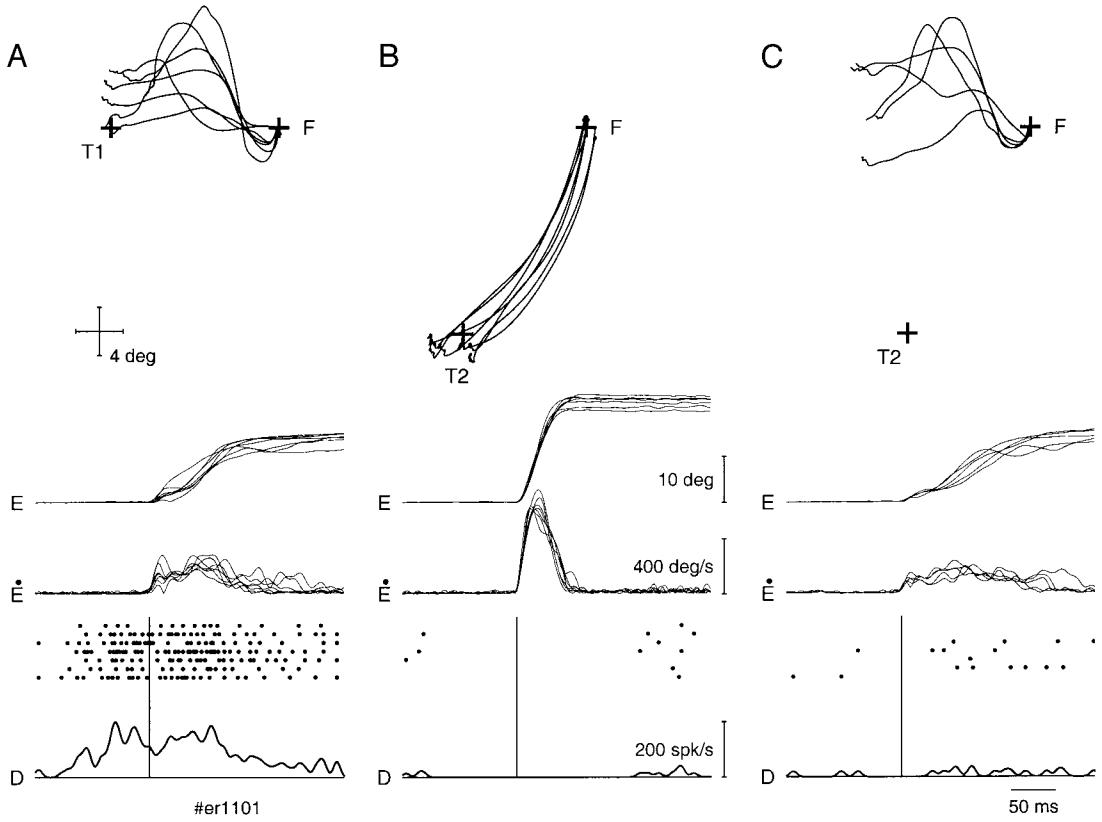

FIG. 15. Goal- and nongoal-directed eye movements, both made into the cell's movement field, resulted in different responses. Data from *cell er1101*. *A*: perturbed, but goal-directed saccades toward flashed targets (T1) presented within the cell's movement field. Note the burst discharge of the cell despite the perturbations. *B*: control saccades toward a target (T2) presented outside the cell's movement field. Note that the cell remains silent. *C*: blink-perturbed saccades showing no compensation, but the resulting eye movements were into the cell's movement field. As in *B*, the animal was required to make saccades toward target T2. Note the absence of a burst discharge despite the similarity between the eye movements in *A* and *C*.

lation was applied in the rostral SC (Munoz et al. 1996) or in the OPN region (Keller and Edelman 1994). In both cases, the observed suppression is thought to result from an inhibition by rostral SC cells that were stimulated either directly (Munoz et al. 1996) or indirectly through retrograde activation (Keller and Edelman 1994). Could it be, therefore, that the blink-related SRBN suppression in the present study was due to an excitation of rostral SC cells? We regard this possibility as unlikely. The rostral zone is involved in active fixation (Munoz and Guitton 1991; Munoz and Wurtz 1993a,b) and has extensive excitatory projections to the OPN region (Büttner-Ennever et al. 1999; Gandhi and Keller 1997; Paré and Guitton 1994). The OPNs, in turn, are known to pause for blinks (Cohen and Henn 1972; Fuchs et al. 1991; Mays and Morrisse 1994). It is more likely, therefore, that rostral SC neurons, like OPNs, will pause for blinks. This would be more in line also with the observed reduction of saccadic latencies (see Goossens and Van Opstal 2000). It is also unlikely that the OPNs would mediate the suppression of SRBN activity since these neurons do not project to the SC (Büttner-Ennever and Büttner 1988).

Resumption of SRBN discharge

The question as to which mechanism underlies the resumption of SRBN activity shortly after blink onset (Fig. 5*B*) cannot be answered on the basis of the present experiments. One possibility could be that an external excitatory signal remains (Munoz et al. 1996). Alternatively, since the suppressive effect of blinking was often far from complete (Fig. 5), it could be that intrinsic properties of the collicular network, such as local excitatory interactions, underlie the resumption of SRBN discharge.

Nevertheless it can be concluded that the resumed discharge was closely linked to the actual oculomotor behavior. First, the (two- to threefold) increase in duration of the perturbed movement was well correlated with the increase in duration of the motor burst (Figs. 6 and 7). Second, despite a substantial reduction in the mean discharge rate, the number of spikes in the burst associated with perturbed saccades was very similar to that in the burst for control saccades (Figs. 8 and 9). Third, the reduction in mean firing rate was well correlated with the reduction in eye velocity during perturbed saccades (Fig. 10). These findings clearly reflect the fact the SRBNs are a major source of input to the brain stem saccade generator. Yet as will be discussed in the following text, these results do not necessarily imply that the SRBNs receive feedback about the saccade trajectory.

Comparison with previous perturbation studies

As reviewed in the INTRODUCTION, previous studies have used electrical microstimulation of either the OPN region (Keller and Edelman 1994) or of the rostral SC (Munoz et al. 1996) to investigate the influence of perturbations in saccade kinematics on the discharge patterns of saccade-related neurons in the SC. These studies revealed a transient cessation in SRBN activity, as well as an intrasaccadic fixation of the eyes. In the case of OPN stimulation, the rostral SC is presumably excited through retrograde activation (Keller and Edelman 1994). Conversely, rostral SC stimulation probably activates also the OPNs (Munoz et al. 1996; Paré and Guitton 1994; Raybourn and Keller 1977). Because of these side effects, it could not be decided whether reactivation of the OPNs or cessation of SRBN activity caused the saccade interruption. As discussed in the preceding text, the air-puff-evoked blinks are instead more likely to cause suppression, rather than excitation, of both the OPNs and the rostral SC in the present experiments. The spatial-temporal saccade disturbances resulting from blinks are also quite different from the brief stimulation-induced saccade interruptions (see Goossens and Van Opstal 2000, for details).

Despite these differences, other aspects of our results are quite comparable with the interruption data. First, SRBNs resumed their discharge also after a blink-induced inhibition although neither the size nor the direction of the compensatory eye movement corresponded to the cell's movement field (e.g., Fig. 11). The latter observation further supports the notion that the saccade trajectory is not encoded by a dynamic shift in the location of activated neurons in the SC motor map (see Anderson et al. 1998). Second, as in the interruption experiments, burst duration remained well coupled to total movement duration (Fig. 7) despite its two- to threefold increase. Third, for both types of perturbations, the total number of spikes in the burst was comparable with that for control responses. Especially for blink-perturbed responses, where the spatial trajectories as well as the movement kinematics were altered much more dramatically, this is quite a remarkable finding. Finally, as was qualitatively observed by Munoz and colleagues, saccade perturbations affected the high-frequency discharge of long-lead (buildup) and short-lead (burst) neurons in a similar way. Our present results confirm and further quantify these observations (Figs. 6, 8, 10, and 13). These data therefore strongly suggest that both SRBN subtypes fulfill very similar roles in the control of saccades. Further support for this hypothesis will be presented in the following text.

Efferent feedback to the motor SC?

FEEDBACK ABOUT THE ACTUAL 2-D TRAJECTORY? One hypothesis about the activity of collicular neurons is that their discharge rate encodes dynamic motor error. This idea was inspired by the observation that the motor burst of many SC neurons ends with saccade offset and that the discharge rate of these cells decays monotonically with radial motor error (Waitzman et al. 1991). As reported by Keller and Edelman (1994) and Munoz et al. (1996), this monotonic decay persists for postinterruption saccades. However, whether these striking properties are due to some form of efferent feedback from the brain stem saccade generator remains difficult to decide on the basis of the interruption data. As argued in the INTRODUCTION, the kinematics of postinterruption saccades are still highly stereotyped as inferred from their main sequence behavior (Munoz et al. 1996). In addition, the saccade trajectories remained unaltered since no changes in movement direction were induced. Thus except for the brief stimulation-induced interruption, the changes in the eye movements were relatively small, whereas the SRBN discharge is typically endowed with a considerable amount of intrinsic noise (see e.g., standard deviations of the control curves in Figs. 12 and 13).

The air-puff-evoked blinks strongly disrupted both the kinematics and the spatial trajectories of saccadic eye movements. Under these conditions, it appeared that the monotonic relation between the SRBN discharge and dynamic motor error was no

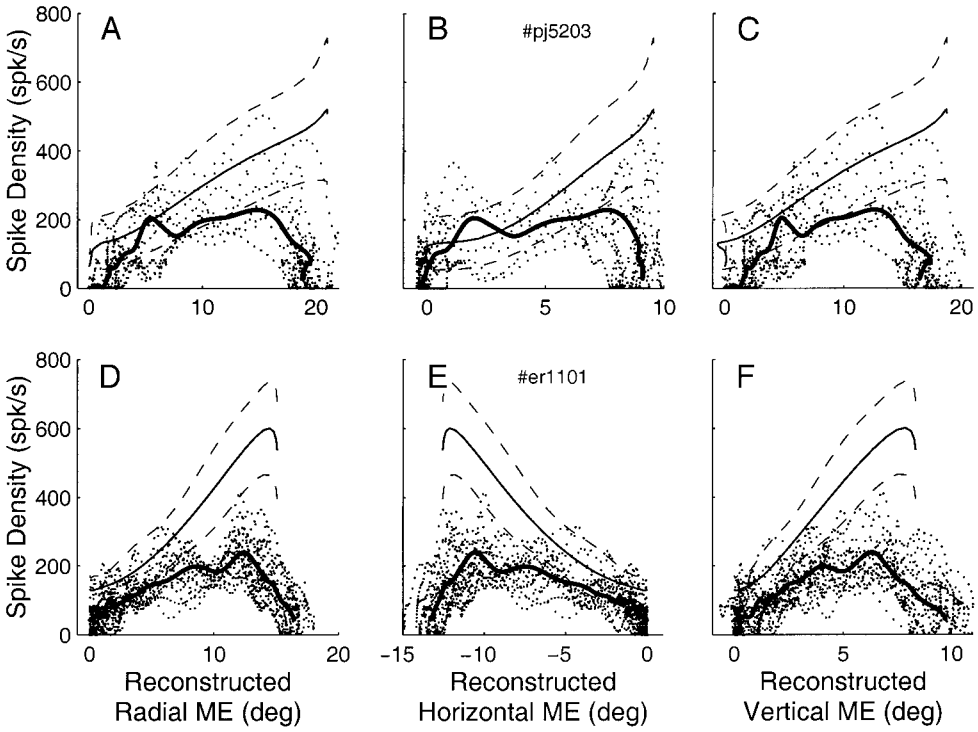

FIG. 16. Spike density as function of dynamic motor error of "reconstructed saccades" for 2 different SRBNs. Reconstructed saccades were obtained by subtracting pure blink-associated eye movements from the blink-perturbed saccades. As shown in the companion paper, the 2-D trajectories of reconstructed saccades were approximately straight, like those of control saccades, but their kinematics were considerably different from the control movements (see Fig. 11 in Goossens and Van Opstal 2000). Same cells, trials and format as in Fig. 13, *A–F*. Note clearly different curves for control saccades (thin curves) and reconstructed saccades (thick curves) in all 6 panels, but qualitatively similar results for the 2 SRBNs.

longer obeyed (Figs. 12 and 13). It should be noted that if the SRBNs were to represent the dynamic motor error signal, the phase relations should have been identical for control and perturbed conditions and the number of spikes in the burst should have increased substantially for perturbed saccades because of their much longer duration. Neither of these requirements were confirmed in our present experiments. Instead it was found that the SRBNs continued their discharge for compensatory movements directed *outside* their movement fields (Fig. 11), while the instantaneous firing rate during such movements could be similar to that during control movements directed *into* the movement field (Fig. 12).

Taken together, our findings indicate that the SRBN discharge rate does not rely on efferent feedback regarding the actual 2-D saccade trajectory. Rather both the blink-induced disturbances as well as the compensatory phase of the eye movement are likely to be generated at a level downstream from the motor SC.

FEEDBACK ABOUT AN INTENDED TRAJECTORY? In the companion paper, we examined the possibility that blink-perturbed saccades result from a linear superposition of two independent motor commands: an unperturbed saccade command and a pure blink-related command. It appeared that the 2-D trajectories, but not the kinematics, of the "reconstructed saccades" (obtained by subtracting pure blink-associated eye movements from blink-perturbed saccades) were comparable with that of control saccades (see Figure 11 in Goossens and Van Opstal 2000). The observation that the reconstructed saccades, like control saccades, had approximately straight trajectories is in line with the results of the present study, which indicate that changes in eye-movement direction are not reflected in the SRBN discharge (Figs. 11 and 12).

It is possible that the SC would only receive dynamic feedback about its own motor command without knowing about the blink-induced trajectory perturbations. Note that this hypothesis would imply that these perturbations occur entirely downstream from this local feedback loop (e.g., at the extraocular motoneurons). If so, phase curves of spike density as function of dynamic motor error of reconstructed saccades would have to be identical to the control curves. However, as illustrated in Fig. 16 (same cells as in Fig. 13, *A–F*), the resulting phase curves were still very different from the control curves. Note that this result follows from the fact that the number of spikes in the burst remained fixed while the dynamics of the reconstructed movements changed considerably.

Number of spikes versus discharge rate

The finding that the number of spikes in the motor burst of collicular SRBNs is roughly invariant to the spatial-temporal properties of the saccade trajectory (Fig. 9) hints at the interesting possibility that this quantity, rather than the firing rate per se, represents the desired eye displacement vector. Recent studies on the effects of electrical microstimulation in the SC also support this hypothesis. By manipulating either stimulation intensity (Van Opstal et al. 1990), or the number of stimulation impulses (Stanford and Sparks 1996), saccade amplitude, but not saccade direction, was systematically varied between zero and the optimal amplitude represented at the stimulation site.

The hypothesis would therefore entail that SRBNs encode a straight eye displacement, the direction of which is determined by the location of the recruited cells within the SC motor map and the movement amplitude of which is determined by the number of spikes in the burst. In this way, the temporal distribution of the SRBN spikes may influence, but not necessarily encode, the velocity of the saccade. A similar suggestion follows from Scudder's model of the collicular-brain stem saccade generator (Scudder 1988).

Note, however, that the amplitude of stimulation-evoked

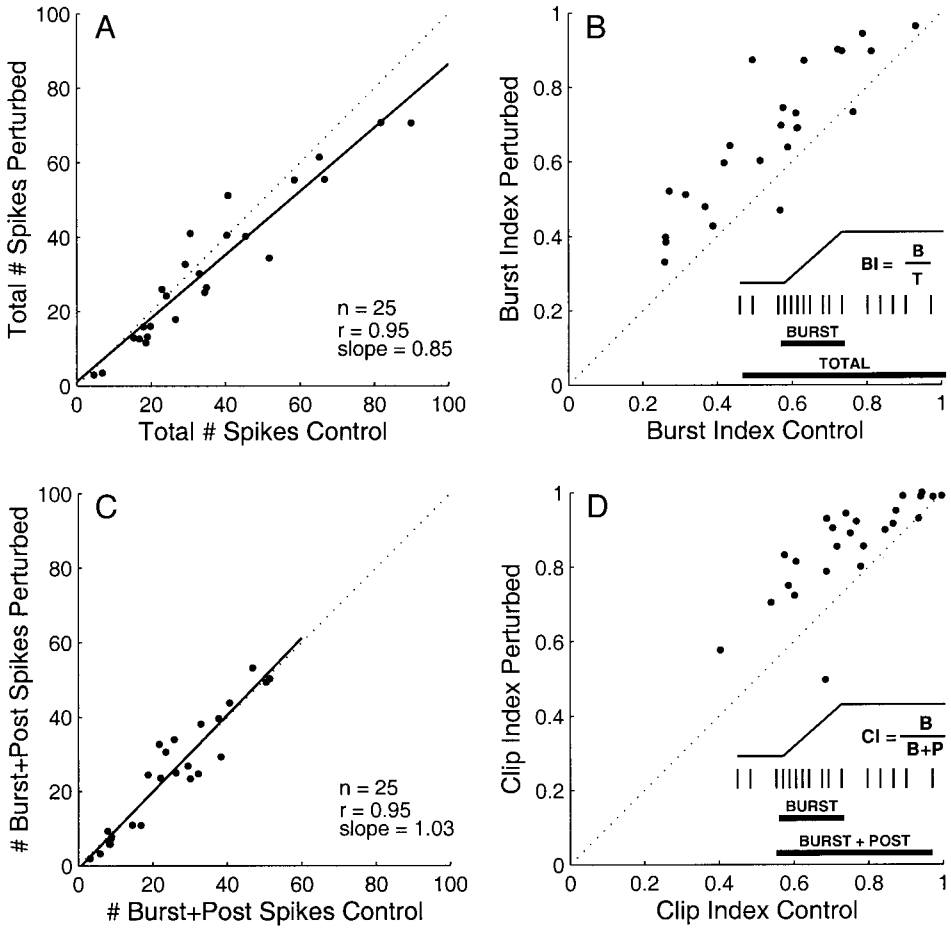

FIG. 17. Spike-count analysis on all 25 fully tested cells. *A*: the total number of spikes, counted in an 800-ms window starting 100 ms after target onset, measured in control trials and perturbation trials was remarkably similar. Slope of the regression line (solid) was slightly different from unity ($P < 0.01$). *B*: the burst index (*BI*) is defined by the number of spikes in the burst, divided by the total number of spikes in the trial shown in A ($BI = B/T$). When $BI = 1.0$, all spikes are contained within the saccade-related burst (burst neuron), low *BI* values refer to neurons with considerable pre- and postsaccadic activity (like buildup cells). Note that *BI* scatters widely over our population of cells and appears to be distributed along a continuum. *C*: the number of spikes in the burst plus the number of postsaccadic spikes was nearly identical in the 2 conditions. Slope of the regression line was not significantly different from 1.00 ($P > 0.1$). *D*: the clip index (*CI*) is defined by the number of spikes in the burst, divided by the number of spikes obtained in the 500-ms window starting 20 ms before saccade onset [Burst + Post; $CI = B/(B + P)$]. For a cell without postsaccadic activity, $CI = 1$, whereas *CI* is very small when the number of postsaccadic spikes far exceeds the burst. The population of cells studied in this paper encompassed a large range of clip indices. Yet all cells exhibit the same properties in their spike counts.

saccades saturates at a site-specific value even if the electric stimulation is continued after the saccade (e.g., Robinson 1972). Similarly the number of spikes in the motor burst is often only a fraction of the total number of spikes (see e.g., Fig. 8), and many SRBNs continue their discharge well after saccade offset (see e.g., Fig. 3). Thus a large proportion of the cells' activity does not contribute directly to the saccade.

To gain further insight into the firing properties of the SRBNs, we have extended our spike-count analysis to include also the pre- and postsaccadic discharge. The results for all 25 fully tested cells are summarized in Fig. 17. Figure 17*A* shows that the total number of spikes (800-ms window; see *inset*), was also very similar for the two experimental conditions for all cells. Figure 17*B* shows the burst index, which we defined as the fraction of spikes in the motor burst relative to the total number of spikes (see *inset*). Note that the burst index is very different from cell to cell (range: 0.25–1.00) and distributed along a continuum. The latter indicates that our cells could not be classified into two separate categories. The spike-count data in Fig. 17*C* evaluate only the burst together with the postsaccadic spikes (500-ms window; see *inset*). Note that in this case the slope of the regression line (solid) is not significantly different from 1.00 ($P > 0.1$) as all data points scatter around the identity line (dashed). This hints at the possibility that the spike count including both burst and postsaccadic activity is the real invariant parameter rather than the saccade-related spike count. Figure 17*D* shows the clip index, which we defined as the fraction of spikes in the motor burst relative to the number of spikes in the burst and postsaccadic activation period (see *inset*), for all 25 cells. A clip index of one indicates no postsaccadic activity, whereas a clip index of zero indicates that there was no burst. Note that the clip indices were slightly different for the two conditions, and in line with Fig. 17*B*, widely distributed (range 0.4–1.0). Thus the tight correlation that is observed in Fig. 17*C* is the same for all SRBNs, regardless of the pre- and postsaccadic discharge properties.

In conclusion, our data suggest that the number of spikes in the motor burst is fixed not because the SRBNs are under feedback control but because intrinsic properties of the SC network ensure that these cells generate a (more than) sufficient number of spikes. This in turn guarantees that the brain stem burst generator can complete the eye displacement vector requested by the SC. This theory implies therefore that a mechanism *downstream* from the SC would count the number of spikes from the SRBN population until a site-specific value is reached, causing reactivation of the OPNs to stop the saccade. Thus the mechanism that apparently determines a fixed number of spikes in the SRBN burst could act entirely downstream from the SC.

Compensatory behavior

Our behavioral data demonstrated that a near-complete compensation for blink-related disturbances ensured that the eye landed close to the extinguished target (see Goossens and Van Opstal 2000). It was argued that this compensatory behavior

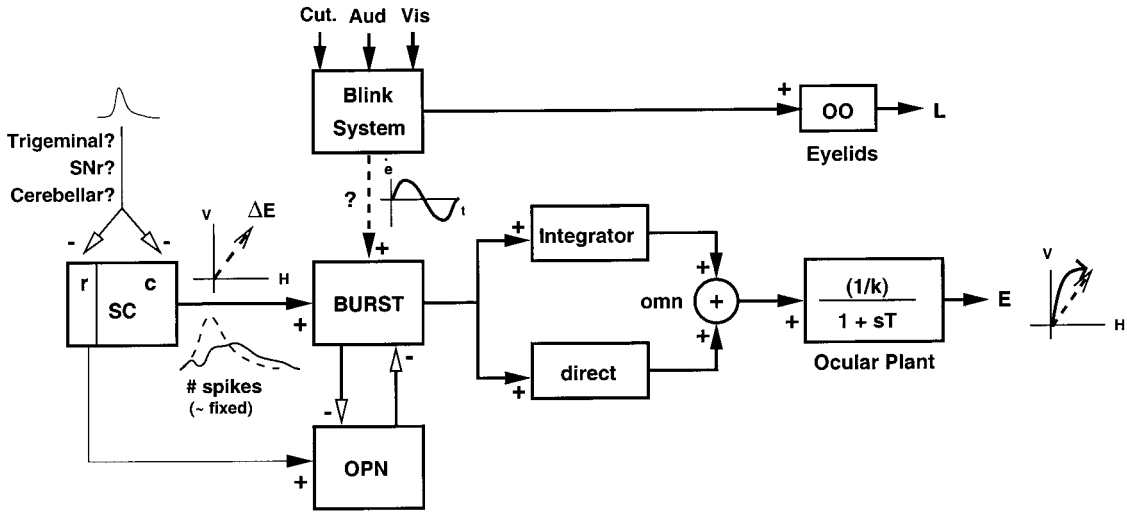

FIG. 18. Conceptual model that may account for the observed phenomena. See DISCUSSION, for explanation. SC, intermediate and deep superior colliculus; BURST, brain stem saccadic burst generator; OPN, omnipause neurons; OMN, extraocular motoneurons; *T* and *k*, time constant and stiffness of the plant; Δ*E*, desired eye displacement; OO, Orbicularis oculi muscle.

was due to neural control mechanisms, rather than to passive elastic restoring forces within the oculomotor plant. Our present neurophysiological data provide strong additional support for this view (e.g., Figs. 1–3 and 14).

Two mechanisms could in principle account for the compensatory movement component: local feedback within the brain stem saccade generator or an active reset eye movement that is generated by the blink system itself. On the basis of the current experiments, it is not possible to decide between either possibility. Local feedback could indeed ensure that the blink-induced eye deflections are automatically corrected for but only if these trajectory perturbations result from a blink-related signal that acts within the local feedback circuit. On the other hand, an active reset movement generated by the blink system itself could be added either to the neural drive from the SC or elsewhere in the premotor circuitry.

It is quite unlikely that the SC mediates the eye-movement deflections since SRBNs are typically suppressed around the onset of a blink (Fig. 5). This is further supported by the data in Figs. 14 and 15, which indicate that only the site corresponding to the desired movement is involved. Instead, we believe that the blink-related signal that is responsible for the 2-D trajectory disturbance interacts with the saccade system at a level that is *downstream* from the SC, but *upstream* from both the extraocular motoneurons and the oculomotor neural integrator. The latter is based on the observation that a blink-associated eye movement often brings the eye to a new orbital position that is maintained until a correction saccade is made (see Goossens and Van Opstal 2000 for examples).

We conjecture, therefore, that blink-associated eye movements may involve neural structures that are parallel to the saccade burst generator but share the oculomotor integrator as well as the omnipause neurons. Alternatively, the blink system could even share also saccadic burst cells in the brain stem. Recordings from burst neurons in the paramedian pontine reticular formation during blinks (Cohen and Henn 1972) have provided preliminary support for the latter possibility.

Conceptual model of saccade-blink interactions

Figure 18 provides a simplified summary scheme of the saccade-blink interactions that may explain the observations from the previous and present paper. In short, when the blink system is activated *1*) motoneurons that innervate the orbicularis oculi muscle (OO) are recruited to produce a blink. *2*) Cells in the entire motor SC are inhibited. As this inhibition gradually subsides, SRBNs at the location corresponding to the overall desired saccade vector resume their activity. Due to remaining suppression, the activity levels in the SRBNs are lower than for control responses. *3*) The saccade burst generator in the brain stem is excited (in this scheme biphasically, to account for the return movement of the eyes as well), which in turn shuts off the omnipause neurons. *4*) Due to this indirect OPN inhibition (possibly combined with inhibition that is more direct), the burst generator is also excited by the SRBNs. Since blink-related and collicular signals add at this level, the resulting eye-movement trajectory is slow and strongly curved but ends close to the target. *5*) SRBNs at a given site in the SC send a burst to the saccade burst generator that contains an approximately fixed number of spikes. *6*) If the number of spikes exceeds a site-specific value, the eye movement will stop by reactivation of the OPNs. This OPN activation ensures that the exact number of spikes produced by the SRBNs is not critical.

We thank C. van der Lee for manufacturing the microelectrodes and H. Kleijnen and T. van Dreumel for technical support. We also thank the staff of the central animal facility for taking care of our monkeys. Dr. F. van der Werf is thanked for helpful discussions and for histology of the recording sites. Both anonymous referees are acknowledged for constructive criticism, which improved the paper substantially.

This research was supported by the Dutch Foundation for the Life Sciences (SLW, project 805-01.072; H.H.L.M. Goossens), the University of Nijmegen (A. J. Van Opstal), and the Human Frontiers Science Program (A. J. Van Opstal; RG0174/1998-B).

Address for reprint requests: H.H.L.M. Goossens, Dept. of Medical Physics and Biophysics, University of Nijmegen, Geert Grooteplein 21, NL-6525 EZ Nijmegen, The Netherlands.

Received 26 March 1999; accepted in final form 16 February 2000.

REFERENCES

ANDERSON RW, KELLER EL, GANDHI NJ, AND DAS S. Two-dimensional saccade-related population activity in superior colliculus in monkey. *J Neurophysiol* 80: 798–817, 1998.

ARAI K, KELLER EL, AND EDELMAN JA. Two-dimensional neural network model of the primate saccadic system. *Neural Networks* 7: 1115–1135, 1994.

BAHILL AT, ADLER D, AND STARK L. Most naturally occurring human saccades have magnitudes of 15°rees or less. *Invest Ophthalmol* 14: 468–469, 1975.

BASSO MA AND EVINGER C. An explanation for blink reflex hyperexcitability in Parkinson's disease. II. Nucleus raphe magnus. *J Neurosci* 16: 7318–7330, 1996.

BASSO MA, POWERS AS, AND EVINGER C. An explanation for blink reflex hyperexcitability in Parkinson's disease. I. Superior colliculus. *J Neurosci* 16: 7300–7317, 1996.

BASSO MA, STRECKER RE, AND EVINGER, C. Midbrain 6-hydroxydopamine lesions modulate blink reflex excitability. *Exp Brain Res* 94: 88–96, 1993.

BECKSTEAD RM, EDWARDS SB, AND FRANKFURTER A. A comparison of the intranigral distribution of nigrotectal neurons labeled with horseradish peroxidase in the monkey, cat, and rat. *J Neurosci* 1: 121–125, 1981.

BERTHOZ A, GRANTYN A, AND DROULEZ J. Some collicular efferent neurons code saccadic eye velocity. *Neurosci Lett* 72: 289–294, 1986.

BOUR LJ, ARAMIDEH M, AND ONGERBOER DE VISSER BW. Neurophysiological aspects of eye and eyelid movements during blinking in humans. *J Neurophysiol* 83: 166–176, 2000.

BOUR LJ, VAN GISBERGEN JAM, BRUIJNS J, AND OTTES FP. The double magnetic induction method for measuring eye movements: results in monkey and man. *IEEE Trans Biomed Eng* 31: 419–427, 1984.

BRONSTEIN AM AND KENNARD C. Predictive ocular motor control in Parkinson's disease. *Brain* 108: 925–940, 1985.

BÜTTNER-ENNEVER J AND BÜTTNER U. The reticular formation. In: *Neuroanatomy of the Oculomotor System*, edited by Büttner-Ennever J. Amsterdam: Elsevier, 1988, p. 119–176.

BÜTTNER-ENNEVER JA, HORN AKE, HENN V, AND COHEN B. Projections from the superior colliculus motor map to omnipause neurons in monkey. *J Comp Neurol* 413: 55–67, 1999.

COHEN B AND HENN V. Unit activity in the pontine reticular formation associated with eye movements. *Brain Res* 46: 403–410, 1972.

COLLEWIJN H, VAN DER MARK F, AND JANSEN TC. Precise recording of human eye movements. *J Neurophysiol* 54: 11–27, 1975.

DAS S, GANDHI NJ, AND KELLER EL. Open-loop simulations of the primate saccade system using burst cell discharge from the superior colliculus. *Biol Cybernet* 73: 509–518, 1995.

DROULEZ J AND BERTHOZ A. A neural network model of sensoritopic maps with predictive short-term memory properties. *Proc Natl Acad Sci USA* 88: 9653–9657, 1991.

EPPING WJ AND EGGERMONT JJ. Coherent neural activity in the auditory mid-brain of the grassfrog. *J Neurophysiol* 57: 1464–1483, 1987.

EVINGER C, BASSO MA, MANNING KA, SIBONY PA, PELLEGRINI JJ, AND HORN AKE. A role for the basal ganglia in nicotinic modulate of the blink reflex. *Exp Brain Res* 92: 507–515, 1993.

EVINGER C, MANNING KA, PELLEGRINI JJ, BASSO MA, POWERS AS, AND SIBONY PA. Not looking while leaping: the linkage of blinking and saccadic gaze shifts. *Exp Brain Res* 100: 337–334, 1994.

EVINGER C, MANNING KA, AND SIBONY PA. Eyelid movements. Mechanisms and normal data. *Invest Ophthalmol Vis Sci* 32: 387–400, 1991.

FUCHS AF. Saccadic and smooth pursuit eye movements in the monkey. *J Physiol (Lond)* 191: 609–631, 1967.

FUCHS AF, LING L, KANEKO CRS, KING WM, AND USHER SD. The timing of the response of brainstem omnipause neurons relative to saccade eye movements in rhesus monkeys. *Soc Neurosci Abstr* 17: 462, 1991.

FISCHER B AND WEBER H. Express saccades and visual attention. *Behav Brain Sci* 16: 553–567, 1993.

GANDHI NJ AND KELLER EL. Spatial distribution and discharge characteristics of superior colliculus neurons antidromically activated from the omnipause region in monkey. *J Neurophysiol* 78: 2221–2225, 1997.

GNADT JW, LU S-M, BREZNEN B, BASSO MA, HENRIQUEZ VM, AND EVINGER C. Influence of the superior colliculus on the primate blink reflex. *Exp Brain Res* 116: 389–398, 1997.

GOOSSENS HHLM AND VAN OPSTAL AJ. Blink-perturbed saccades in monkey. I. Behavioral analysis. *J Neurophysiol* 83: 3411–3429, 2000.

GOOSSENS HHLM, VAN OPSTAL AJ, AND GIELEN CCAM. Superior colliculus activity during saccadic eye movements perturbed by air-puff induced blinks. *Soc Neurosci Abstr* 22-I: 663, 1996.

GOOSSENS HHLM, HOFMAN PM, AND VAN OPSTAL AJ. Inferior colliculus activity in the awake and behaving monkey. *Soc Neurosci Abstr* 23-I: 735, 1997.

GRAYBIEL A. Organization of the nigrotectal connection: an experimental tracer study in the cat. *Brain Res* 143: 339–348, 1978.

GRUART A AND DELGADO-GARCÍA JM. Signalling properties of identified deep cerebellar nuclear neurons related to eye and head movements in the alert cat. *J Physiol (Lond)* 478: 37–54, 1994.

HIKOSAKA O AND WURTZ RH. Visual and oculomotor functions of monkey substantia nigra pars reticulata. I. Relation of visual and auditory responses to saccades. *J Neurophysiol* 49: 1230–1253, 1983.

HUERTA MF, FRANKFURTER AJ, AND HARTING JK. The trigeminocollicular projection in the cat: patch-like endings within the intermediate gray. *Brain Res* 211: 1–13, 1981.

HUERTA MF, FRANKFURTER A, AND HARTING JK. Studies of the principal sensory and spinal trigeminal nuclei of the rat: projections to the superior colliculus, inferior olive, and cerebellum. *J Comp Neurol* 220: 147–167, 1983.

JÜRGENS R, BECKER W, AND KORNHUBER HH. Natural and drug-induced variations of velocity and duration of human saccadic eye movements: evidence for a control of the neural pulse generator by local feedback. *Biol Cybernet* 39: 87–96, 1981.

KELLER EL AND EDELMAN JA. Use of interrupted saccade paradigm to study spatial and temporal dynamics of saccadic burst cells in the superior colliculus in monkey. *J Neurophysiol* 72: 2754–2770, 1994.

LEE C, ROHRER WH, AND SPARKS DL. Population coding of saccadic eye movements by neurons in the superior colliculus. *Nature* 332: 357–360, 1988.

LEFÈVRE P AND GALIANA HL. Dynamic feedback to the superior colliculus in a neural network model of the gaze control system. *Neural Networks* 5: 871–890, 1992.

LEIGH RJ, NEWMAN SA, FOLSTEIN SE, LASKER AG, AND JENSEN BA. Abnormal ocular motor control in Huntington's disease. *Neurology* 33: 1268–1275, 1983.

MACPHERSON JM AND ALDRIDGE JW. A quantitative method of computer analysis of spike train data collected from behaving animals. *Brain Res* 175: 183–187, 1979.

MAY PJ AND HALL WC. The sources of the nigrotectal pathway. *Neuroscience* 19: 159–180, 1986.

MAY PJ, HARTWICH-YOUNG R, NELSON J, SPARKS DL, AND PORTER JD. Cerebellotectal pathways in the macaque: implications for collicular generation of saccades. *Neuroscience* 36: 305–324, 1990.

MAYS LE AND MORRISSE DW. Activity of pontine omnipause neurons during eye blinks. *Soc Neurosci Abstr* 20: 1404, 1994.

MAYS LE AND SPARKS DL. Dissociation of visual and saccade-related responses in superior colliculus neurons. *J Neurophysiol* 43: 207–232, 1980.

MCHAFFIE JG, KAO C, AND STEIN BE. Nociceptive neurons in rat superior colliculus: response properties, topography and functional implications. *J Neurophysiol* 62: 510–525, 1989.

MCILWAIN JT. Lateral spread of neural excitation during microstimulation in the intermediate gray layer of cat's superior colliculus. *J Neurophysiol* 45: 167–178, 1982.

MOSCHOVAKIS AK AND HIGHSTEIN SM. The anatomy and physiology of primate neurons that control rapid eye movements. *Annu Rev Neurosci* 17: 465–488, 1994.

MUNOZ DP AND GUITTON D. Control of orienting gaze shifts by the tectoreticulospinal system in head-free cat. II. Sustained discharges during motor preparation and fixation. *J Neurophysiol* 66: 1624–1641, 1991.

MUNOZ DP, PÉLISSON D, AND GUITTON D. Movement of neural activity on the superior colliculus map during gaze shifts. *Science* 251: 1358–1360, 1991.

MUNOZ DP, WAITZMAN DM, AND WURTZ RH. Activity of neurons in monkey superior colliculus during interrupted saccades. *J Neurophysiol* 75: 2562–2580, 1996.

MUNOZ DP AND WURTZ RH. Fixation cells in the monkey superior colliculus. I. Characteristics of cell discharge. *J Neurophysiol* 70: 576–589, 1993a.

MUNOZ DP AND WURTZ RH. Fixation cells in the monkey superior colliculus. II. Reversible activation and deactivation. *J Neurophysiol* 70: 576–589, 1993b.

MUNOZ DP AND WURTZ RH. Saccade-related activity in monkey superior colliculus. I. Characteristics of burst and buildup cells. *J Neurophysiol* 73: 2313–2333, 1995.

OPTICAN LM. A field theory of saccade generation: temporal-to-spatial transformation in the superior colliculus. *Vision Res* 35: 2213–3320, 1995.

OTTES FP, VAN GISBERGEN JAM, AND EGGERMONT JJ. Visuomotor fields of the superior colliculus: a quantitative model. *Vision Res* 12: 1795–1808, 1986.

PARÉ M AND GUITTON D. The fixation area of the cat superior colliculus: effects of electrical stimulation and direct connections with brainstem omnipause neurons. *Exp Brain Res* 101: 109–122, 1994.

RASCOL O, CLANET M, MONTASTRUC JL, SIMONETTA M, SOULIER-ESTEVE MJ, DOYON B, AND RASCOL A. Abnormal ocular movements in Parkinson's disease. Evidence for involvement of dopaminergic systems. *Brain* 112: 1193–1214, 1989.

RAYBOURN MS AND KELLER EL. Colliculoreticular organization in primate oculomotor system. *J Neurophysiol* 40: 861–878, 1977.

REDGRAVE P, MCHAFFIE JG, AND STEIN BE. Nociceptive neurones in rat superior colliculus. I. Antidromic activation from the contralateral predorsal bundle. *Exp Brain Res* 109: 185–196, 1996.

RICHMOND BJ AND OPTICAN LM. Temporal encoding of two-dimensional patterns by single units in primate inferior temporal cortex. II. Quantification of response wave form. *J Neurophysiol* 57: 147–161, 1987.

ROBINSON DA. Eye movements evoked by collicular stimulation in the alert monkey. *Vision Res* 12: 1795–1808, 1972.

SCHILLER PH AND STRYKER M. Single-unit recording and stimulation in superior colliculus of the alert rhesus monkey. *J Neurophysiol* 35: 915–924, 1972.

SCUDDER CA. A new local feedback model of the saccadic burst generator. *J Neurophysiol* 59: 1455–1475, 1988.

SNIDER RS AND LEE JC. *A Stereotaxic Atlas of the Monkey Brain (Macaca mulatta).* Chicago, IL: Univ. of Chicago Press, 1961.

SPARKS DL AND HARTWICH-YOUNG R. The deep layers of the superior colliculus. In: *The Neurobiology of Saccadic Eye Movements, Reviews of Oculomotor Research,* edited by Wurtz RH and Goldberg ME. Amsterdam: Elsevier, 1989, vol. III, p. 213–256.

SPARKS DL AND MAYS LE. Movement fields of saccade-related burst neurons in the monkey superior colliculus. *Brain Res* 113: 21–34, 1980.

STANFORD TR, FREEDMAN EG, AND SPARKS DL. Site and parameters of microstimulation: evidence for independent effects on the properties of saccades evoked from the primate superior colliculus. *J Neurophysiol* 76: 3360–3381, 1996.

VAN GISBERGEN JAM, ROBINSON DA, AND GIELEN S. A quantitative analysis of generation of saccadic eye movements by burst neurons. *J Neurophysiol* 45: 417–442, 1981.

VAN OPSTAL AJ AND GOOSSENS HHLM. Superior colliculus activity during blink-perturbed saccades: implications for saccade control models. *Soc Neurosci Abstr* 25-II: 1922, 1999.

VAN OPSTAL AJ AND KAPPEN H. A two-dimensional ensemble coding model for spatial-temporal transformation of saccades in monkey superior colliculus. *Network* 4: 19–38, 1993.

VAN OPSTAL AJ AND VAN GISBERGEN JAM. Role of monkey superior colliculus in saccade averaging. *Exp Brain Res* 79: 143–149, 1990.

VAN OPSTAL AJ, VAN GISBERGEN JAM, AND SMIT AC. Comparison of saccades evoked by visual and collicular electrical stimulation in the alert monkey. *Exp Brain Res* 79: 299–312, 1990.

WAITZMAN DM, MA TP, OPTICAN LM, AND WURTZ RH. Superior colliculus neurons mediate the dynamic characteristics of saccades. *J Neurophysiol* 66: 1716–1737, 1991.

WHITE OB, SAINT-CYR JA, TOMLINSON RD, AND SHARPE JA. Ocular motor deficits in Parkinson's disease. II. Control of the saccadic and smooth pursuit systems. *Brain* 106: 571–587, 1983.

WIBERG M, WESTMAN J, AND BLOMQVIST A. Somatosensory projection to the mesencephalon: an anatomical study in the monkey. *J Comp Neurol* 264: 92–117, 1987.

WURTZ RH AND OPTICAN LM. Superior colliculus cell types and models of saccade generation. *Curr Opin Neurobiol* 4: 857–861, 1994.

ZEE DS, CHU FC, LEIGH RJ, SAVINO PJ, SCHATZ NJ, REINGOLD DB, AND COGAN DG. Blink-saccade synkinesis. *Neurology* 33: 1233–1236, 1983.